Skew Surge and Storm Tides of Tropical Storms in the Delaware and Chesapeake Bays for 1980 - 2019

John A. Callahan[1*], Daniel J. Leathers[2], Christina L. Callahan[2]

[1]Delaware Geological Survey, Department of Geography and Spatial Sciences, University of Delaware, Newark, Delaware, USA

[2]Department of Geography and Spatial Sciences, Center for Environmental Monitoring & Analysis, University of Delaware, Newark, Delaware, USA

*** Correspondence:**
Corresponding Author
john.callahan@udel.edu

Keywords: tropical cyclones, hurricanes, storm surge, coastal flooding, flood risk, Mid-Atlantic, tidal analysis

Abstract

Coastal flooding poses the greatest threat to human life and is often the most common source of damage from coastal storms. From 1980 to 2020, the top 6, and 17 of the top 25, costliest natural disasters in the U.S. were caused by coastal storms, most of these tropical systems. The Delaware and Chesapeake Bays, two of the largest and most densely populated estuaries in the U.S. located in the Mid-Atlantic coastal region, have been significantly impacted by strong tropical cyclones in recent decades, notably Hurricanes Isabel (2003), Irene (2011), and Sandy (2012). Current scenarios of future climate project an increase in major hurricanes and the continued rise of sea levels, amplifying coastal flooding threat. We look at all North Atlantic tropical cyclones (TC) in the International Best Track Archive for Climate Stewardship (IBTrACS) database that came within 750 km of the Delmarva Peninsula from 1980 to 2019. For each TC, skew surge and storm tide are computed at 12 NOAA tide gauges throughout the two bays. Spatial variability of the detrended and normalized skew surge is investigated through cross-correlations, regional storm rankings, and comparison to storm tracks. We find Hurricanes Sandy (2012) and Isabel (2003) had the largest surge impact on the Delaware and Chesapeake Bay, respectively. Surge response to TCs in upper and lower bay regions are more similar across bays than to the opposing region in their own bay. Distance from Delmarva and relative location of storm track play a role in the magnitude and variability of surge, although distance itself is not a strong predictor. TCs that impacted lower bay more than upper bay regions tended to stay offshore east of Delmarva, whereas TCs that impacted upper bay regions tended to stay to the west of Delmarva. Although tropical cyclones are multi-hazard weather events, there continues to be a need to improve storm surge forecasting and implement strategies to minimize the damage of coastal flooding. Results from this analysis can provide insight on the potential regional impacts of coastal flooding from tropical cyclones in the Mid-Atlantic.

1 Introduction

Coastal storms are a multi-threat natural hazard, often including heavy rain, strong winds, large waves, rip currents, and storm surge, all of which must be considered collectively when assessing risk and devising mitigation strategies. According to the National Oceanic and Atmospheric Administration (NOAA), for the years 1980 – 2019, 17 of the top 25 costliest natural disasters in the US were caused by tropical cyclones (TCs) (NCEI, 2020). Coastal flooding, primarily from storm surge and waves, from these storms poses the greatest threat to human life and is often the source of much of the damage (Blake and Gibney, 2011; Rappaport, 2014; Chippy and Jawahar, 2018; Weinkle et al., 2018).

Two of the largest estuaries in the United States, the Delaware and Chesapeake Bays, have been significantly impacted by strong TCs in recent decades, notably Hurricanes Sandy (2012), Irene (2011) and Isabel (2003). These two estuaries, located in the Mid-Atlantic coastal region, house approximately 27 million inhabitants, a high density of metropolitan areas, transportation networks, industrial ports, and currently are under active development (Sanchez et al., 2012; Chesapeake Bay Program, 2020). Alongside large investments in public and private infrastructure, the region also hosts numerous critical natural ecosystems, saltmarshes and freshwater wetlands, agricultural fields, and forested lands threatened by degradation and erosion. Coastal flooding has been deemed an important natural hazard in this region (DEMA, 2018; Boesch et al., 2018) and can have a tremendous economic impact on current and future waterfront areas (Li et al., 2020).

Impacts from coastal flooding are highly dependent upon both the natural and social vulnerability of a location (i.e., it is hyper-local), as well as the human response to implement adaptation measures (e.g., dune/berm systems, shoreline hardening), and therefore can vary drastically over short distances. The wide diversity of land use and vulnerable communities make it difficult to plan for this region as a whole. It is critical that we understand the severity and geographic variability of storm surge to properly assess the risk, aid in preparedness, and ultimately reduce the severe impacts from coastal flooding (CCPR, 2016).

Water levels in the Delaware and Chesapeake Bays have been well monitored by tide-gauge networks for several decades, particularly at NOAA National Water Level Observation Network (NWLON) sites operated through the Physical Oceanographic Real-Time System (PORTS) for each bay. Although this is primarily due to the importance of marine navigation and public safety, many of these gauges are particularly high quality, have very long records, and have been well-cited for monitoring sea-level rise and climate studies (Holgate et al., 2013; Sweet et al., 2017a; NOAA PORTS, 2020; NOAA NWLON, 2020). Relative sea-level rise (SLR) (Sallenger et al., 2012; Kopp, 2013; Boon et al., 2018) and high-tide flooding (Sweet et al., 2014; Sweet et al., 2020) rates in the region have increased in recent decades as compared to the early-mid 20th Century and are expected to continue increasing into the near future (Callahan et al., 2017; Boesch, et al. 2018; Sweet et al., 2017a). Increases in sea levels lead directly to higher probabilities of coastal flood events (Rahmstorf, 2017; Sweet et al., 2017b).

The Mid-Atlantic region lies in a climatic transition zone, between continental and marine climate types, split in the Fourth National Climate Assessment (Jay et al., 2018) between the Northeast (Delaware Bay and upper Chesapeake Bay) and the Southeast (lower Chesapeake Bay) Regions. Mid-Atlantic weather is often dictated by the relative position of the westerly polar jet stream (often times directly above in the winter), flanked by baroclinic instability from warm ocean waters to the east and atmospheric uplift along the Appalachian front to the west (Leathers et al., 1998; Strobach et al, 2018). Coastal flooding is observed year-round from East Coast winter storms (Hirsch et al, 2000) , , surface high pressure systems (spring to fall) and tropical systems (summer to fall), with a higher percentage of TC-caused extreme flood events in the southern portions of the region (Booth et al., 2016). Although the Mid-Atlantic has been impacted by tropical systems less frequently than some other portions of the U.S., recent tropical cyclones and their associated storm surge and river flooding have caused damages in excess of $80 billion (Smith and Katz, 2013), hundreds of injuries, and loss of life across this heavily populated and economically sensitive region of the country.

Several climatologies of tropical weather systems and their impacts have been completed for the Atlantic and Gulf coast regions of the U.S. (i.e. Simpson and Lawrence, 1971; Landsea and Franklin, 1993; Elsner and Kara, 1999; Muller and Stone, 2001; Xie et al., 2005; Keim et al., 2007; McAdie et al., 2009). Results from these studies (Keim et al., 2007) indicate that the Mid-Atlantic experiences return periods of 4 – 10 years for any tropical cyclone (including tropical storms and hurricanes), 35 – 100 years for hurricanes of any strength, and greater than 100 years for Category 3 and above hurricanes. These return periods are significantly longer than other areas along the Atlantic and Gulf coasts of the U.S., due mainly to the inland position of the Mid-Atlantic coastline.

In additions to sea levels, sea-surface temperatures (SSTs) in the equatorial and North Atlantic are also expected to increase under future global warming scenarios, leading to an increase in the number of severe tropical cyclones (Kossin et al., 2017; Knutson et al., 2020). Recent research has also shown trends in tropical cyclone location moving northward, increases in rapid intensification and surface wind speeds, and decrease in translational speed (Kossin, 2018; Knutson et al., 2019; Murakami et al., 2020; Yang et al., 2020). All of these suggest the extreme importance to understand current and past coastal flooding due to TCs.

Numerous studies have utilized storm surge to measure frequency or impact of coastal storms along the US Atlantic Coast (Dolan and Davis, 1992; Zhang, 2000; Bernhardt and DeGaetano, 2012; Colle et al., 2015) or globally (Marcos et al., 2015; Mawdsley et al., 2016). However, few have focused on tropical systems occurring in the Delaware and Chesapeake Bays, or the Mid-Atlantic in general.

SURGEDAT is a database specifically designed to store storm surge data. It contains 700 tropical surge events around the world and more than 8,000 unique tropical high-water marks along the U.S. Gulf and Atlantic Coasts since 1880, however, only a few records are located in the Mid-Atlantic region (Needham et al., 2015). The USACE North Atlantic Comprehensive Coastal Survey report (USACE, 2014) and FEMA Region 3 Coastal Storm Surge Study (FEMA, 2013) included many simulated tropical systems in their storm surge modeling work due to the dearth of observational data in the region. Booth et al. (2016) looked at all extreme storm surge events and the relative influence of tropical cyclones for select gauges in the Mid-Atlantic. They found that for large coastal flood events, tropical systems were the most likely cause, whereas for less severe events, the relative importance of tropical systems decreased, and extratropical cyclones increased. Wilkerson and Brubaker (2013) investigated the spatial variability of storm surge in the lower Chesapeake Bay over all extreme coastal flooding events but included only a few tropical cyclones. Rashid et al. (2019) looked at interannual and multi-decadal variability of extreme storm surge during the peak extratropical (November – April) and tropical (May – October) seasons. Although they included surges from all types of storm events, they concluded that the Mid-Atlantic region varied differently than the Northeast and Southeast portions of the U.S. Atlantic Coast at long time scales.

The overall goal of the current study is to improve understanding of the magnitude and spatial variability of tropical cyclone-caused coastal flooding in the Delaware and Chesapeake Bays. The first part of the paper focuses on the computation of skew surge at tide gauges for each TC event. Skew surge is not commonly used to assess the surge produced by a storm although it may be a more appropriate measure of risk of storm surge (refer to Section 2.4 for more details). The remaining parts of the paper focus on grouping tide gauges with similar skew surge response into sub-bay geographic regions, as well as grouping TCs into clusters that exhibit similar spatial patterns of skew surge. This information will aid in local planning, emergency preparedness, and communication outreach regarding the hazards of coastal storms in the region.

2 Materials and Methods

2.1 Study Region

The Delaware and Chesapeake Bays, connected via the Chesapeake and Delaware (C & D) Canal, surround the Delmarva Peninsula (Figure 1). Both bays are heavily tidally influenced with freshwater inputs from the major river systems of the Delaware River, Susquehanna River, and Potomac River. Tidal water levels are impacted by many environmental characteristics, including the geometry of the coastline, bathymetry, bottom friction/dissipation effects, reflection of the wave near the head of the bay (Lee et al., 2017) as well as prevailing remote winds and ocean currents. Storm surge, while also impacted by these factors, is additionally influenced by characteristics of the storm itself, such as storm size and direction of travel, duration, atmospheric pressure, wind speed and wind direction relative to the coastline (Ellis and Sherman, 2015). Coastal flood levels in this region are the net effect of numerous complex hydrodynamics at play.

The Delaware Bay has a classical funnel shape, width of about 18 km at its mouth between Cape Henlopen and Cape May, expanding to approximately 45 km at its widest point (Wong and Münchow, 1995), with an average bathymetry of about 7 m, although deep scour in the middle of the lower part of the bay can extend to over 20 – 25 m (Eagleson and Ippen, 1966; Harleman 1966; Salehi, 2018). The converging coastlines toward the head of the bay amplifies tides in the northern regions, where the tidal range is over 2 m compared to less than 1.5 m near the mouth (Lee et al., 2017; Ross et al, 2017). This contrasts with the Chesapeake Bay, a much longer bay, more dendritic in form with many tributaries, ranging in width from 5.6 to 56 km. The Chesapeake Bay is relatively shallow at median depth of about 6 m, with only 18% of its surface area at depths above 12 m, although a narrow navigation channel width depths > 9 m exists along the east side of the main channel (Patrick, 1994; Xiong and Berger, 2010). Tidal range is approximately 0.7 m in the northern reaches, dipping to 0.3 m at the middle of the bay, increasing to 0.9 m at the mouth (Zhong and Li, 2006; Lee at al., 2017; Ross et al., 2017).

Tidal cycle patterns in this region are mainly semi-diurnal, albeit the tides transition in the Chesapeake Bay from semi-diurnal in the lower portion to a mixed tidal regime in the upper portions, forming a mix of progressive and standing waves throughout the bay system (Xiong and Berger, 2010; Ross, 2017). The average seasonal cycle of mean sea level is similar across the bays, a bimodal distribution with the maximum in fall (October) and secondary maximum in late spring (May-June), primarily caused by periodic fluctuations in atmospheric weather systems and coastal water steric effects (COOPS, 2020a).

2.2 Tropical Cyclone Data

Tropical cyclone information used in this study is extracted from the International Best Track Archive for Climate Stewardship (IBTrACS) North Atlantic Basin dataset Version 4 (Knapp et al., 2018). IBTrACS is a collection of global best track data for cyclones that achieved tropical or sub-tropical status at some point in their lifetime. Data were obtained from multiple research centers around the world and are stored in a centralized location for standardized distribution (Knapp et al., 2010). IBTrACS has been endorsed by the World Meteorological Organization non-government domain Tropical Cyclone Programme as an official archiving and distribution resource for tropical cyclone best track data.

For the current study, TCs were limited to those occurring in the North Atlantic Ocean basin during the time period 1980 – 2019 with tracks that cross within a 750 km radius circular buffer of the Delmarva Peninsula. The large 750 km radius, relative to the typical size of TCs, was chosen to be sure to capture TCs that could significantly impact water levels (Zhang et al., 2000; Booth et al., 2016). Distance to Delmarva was calculated as the great circle distance using the GRS80 reference ellipsoid from the TC center to a reference location along the Delmarva coastline for each 3-hour record within IBTrACS. The Delmarva coastal reference point, which also serves as the center of the 750 km circular buffer, was determined by computing the mean latitude and longitude coordinates of the six coastal tide gauges used in the study, namely Atlantic City (ATL), Cape May (CAP), Lewes (LEW), Wachapreague (WAC), Kiptopeke (KIP), and Sewells Point (SEW) (Figure 1; Table 1). This resulted in a subset of 144 TCs with median annual count of 3.5 TCs. The monthly distribution closely matches, although occurring slightly earlier in the season, the distribution of all North Atlantic TCs (Figure 2). However, the annual percentage of all North Atlantic TCs that are near Delmarva can be quite variable, with a minimum of 5% in 2010 and a maximum of 50% occurring in 1985 and 2004.

IBTrACS notes the original source of information for each storm record. The data source for all the selected TCs from 1980 through 2018 is the U.S. National Hurricane Center (NHC) Hurricane Database 2 (HURDAT2) (Landsea and Franklin, 2013). TCs from the 2019 season were listed as NHC provisional status and likely were the operational best track estimate (i.e., have not yet been reanalyzed post-season). Specific data retained from the IBTrACS dataset include the TC name and storm ID, center latitude and longitude, date and time, and storm status (e.g., hurricane, tropical storm, tropical disturbance). Although HURDAT2 records correspond to 00, 06, 12, and 18Z times, IBTrACS interpolates many variables to 3-hourly observations using splines for positional data or linearly for non-positional data. GIS shapefiles of storm tracks were also obtained from IBTrACS.

2.3 Water Level Data

Tide gauges selected for this study were limited to NOAA operational tide gauges in and immediately around the Delaware and Chesapeake Bays. Requirements were that the gauge maintained nearly continuous record of hourly water levels for the time period 1980 – 2019, evenly located throughout the region, a set of harmonic constituents identified for making tidal predictions, and a vertical tidal datum conversion factor to North American Vertical Datum of 1988 (NAVD88). In all, 12 gauges were selected; 5 associated with the Delaware Bay and 7 with the Chesapeake (Figure 1; Table 1). All selected gauges are part of NOAA NWLON and PORTS networks.

Table 1. *Tide gauges used in the current study. Number of data gaps and percent hourly data based upon time period 1980 – 2019. Data gaps represent continuous gaps of 745 hours or more. Number of missing tropical cyclones (TCs) is based on the 144 North Atlantic TCs that crossed into the 750 km buffer around Delmarva over the same time period.*

Station	Abbr.	NOAA ID	Bay	Coordinates	Data Gaps	Percent Hourly	Missing TCs
Philadelphia	PHL	8545240	Delaware	39.933000, -75.142667	0	99.23%	0
Reedy Point	RDY	8551910	Delaware	39.558333, -75.573333	5	95.61%	2
Lewes	LEW	8557380	Delaware	38.781667, -75.120000	0	99.73%	1
Cape May	CAP	8536110	Delaware	38.968333, -74.960000	2	98.35%	0
Atlantic City	ATL	8534720	Delaware	39.356667, -74.418333	2	98.08%	1
Baltimore	BAL	8574680	Chesapeake	39.266667, -76.580000	0	99.66%	1
Annapolis	ANN	8575512	Chesapeake	38.983333, -76.481667	1	98.70%	1
Cambridge	CAM	8571892	Chesapeake	38.571667, -76.061667	1	98.84%	1
Lewisetta	LWS	8635750	Chesapeake	37.995000, -76.465000	2	98.72%	1
Kiptopeke	KIP	8632200	Chesapeake	37.165000, -75.988333	0	99.78%	3
Sewells Point	SEW	8638610	Chesapeake	36.946667, -76.330000	0	100.00%	0
Wachapreague	WAC	8631044	Chesapeake	37.608333, -75.685000	6	89.30%	11

Hourly and High/Low water level data were downloaded from NOAA Center for Operational Oceanographic Products and Services (CO-OPS) API for Data Retrieval (CO-OPS, 2020b). High/Low data represent the exact time and magnitude of each Higher-High, High, Low, and Lower-Low tidal peak. Hourly data represent the observed water level on each hour (e.g., 21:00, 22:00). The 40 years of hourly data at each gauge were manually inspected for errors and inconsistencies. Small periods of data clusters (2 – 16 hours) were removed from the hourly time series (on seven occasions across all gauges) that existed within larger time periods of missing data to better represent the number and length of existing data gaps. No data from the High/Low time series were removed. Data gaps of 1 or 2 hours (less than 10 across all gauges) were filled using linear interpolation. Larger data gaps were not filled. Table 1 lists the number of data gaps that spanned 745 hours (approximately 1 month) or greater as well as the percentage of valid hourly data points. Reedy Point and Wachapreague had the highest number of large data gaps, five and six, respectively, and lowest percentage of valid hourly data (based on a maximum of 14610 hours during 1980 – 2019), 95.61% and 89.30%, respectively. Water level records were compared against the dates of the TCs while within the 750 km buffer of Delmarva. Very few of the 144 TCs were missing from the water level records. Wachapreague had the largest amount of missing data due to a 2.5-year period (200511 – 200804) when valid Hourly and High/Low data were unavailable.

2.4 Skew Surge and Harmonic Analysis

This study uses skew surge as the measure of flooding contributed by each tropical storm. Skew surge is defined as the difference between the maximum observed total water level and the maximum predicted tidal level during a tidal cycle, even if the observed and predicted tidal peaks are offset (i.e., skewed) from each other (Figure 3; Pugh and Woodworth, 2014). Each tidal cycle therefore has one value of skew surge. By measuring the height of water levels above highest predicted tide, skew surge represents the increase of water levels more clearly separated from the astronomically forced-tides and tide-surge interactions (Batstone, 2013; Mawdsley and Haigh, 2016; Williams et al., 2016; Stephens et al., 2020). With respect to preparedness, skew surge represents a truer estimate of the amount of water a location observes above what they expected from high tides alone. Hourly non-tidal residual (NTR, the difference between coincident total water level and predicted tide) is a more common measure of storm surge. However, the statistically computed hourly NTR includes known and unknown non-linear interactions between tides and low-frequency surge produced by a storm, which are complex and dependent upon many environmental factors (Bernier et al., 2007; Spicer et al., 2017). As well, often during coastal flooding storm events, the maximum NTR does not coincide exactly with predicted high tide peak e.g., Hurricane Ernesto 2006 at Sewells Point and Hurricane Sandy 2012 at Reedy Point tide gauges had their largest residuals occur near predicted low tide. Overall, skew surge is less dependent upon tide-surge interactions and independent of tidal phase, proving to be advantageous in developing joint probability estimates of extreme water levels for long-term planning, and therefore less prone to misleading conclusions drawn from NTR estimates of surge (Williams et al., 2016).

Predicted tides were computed at each gauge through harmonic analysis based on hourly total water level time series using the U-Tide Matlab software package (Codiga, 2011). Harmonic analysis incorporated the set of 37 harmonic constituents defined by NOAA for their official tide predictions in this region (CO-OPS, 2020c). This set of 37 constituents are based on known astronomically-cyclic motions of the Earth-Sun-Moon system and local resonances due to water depth and geomorphology of the region that are tidally significant; other tidal constituents were either too small a magnitude or too long a period (i.e., multiple years) to significantly alter daily tidal predictions (NOAA CO-OPS email communication, 2019). Additionally, the seven constituents noted by Harris (1991) relevant for US East Coast water levels were included in the harmonic analysis. The same set of 44 constituents were used for all tide gauges. A lowpass filter was not applied to the hourly NTR as this could also remove meteorological forcing on water levels at these frequencies, which occur when tropical systems move quickly through the Mid-Atlantic region on the order of a tidal cycle or less.

Harmonic analysis was performed in 1-year segments over each calendar year (Jan – Dec) instead of on the full 40-year time period simultaneously. For time periods with data gaps of 1 month or larger, the harmonic analysis was performed on a 3-year period, centered on the year with most missing data, to ensure capture of the seasonal variation. Annual computations minimizes timing errors that can lead to the leakage of tidal energy into the nontidal residual (Merrifield et al., 2013) and minimizes the impact of sea-level rise as the increasing trend is absorbed into the model through the annual mean. Moreover, a 40-year analysis would have resulted in harmonics fit to average conditions and therefore would not account for changing constituent magnitudes that could result from deepening water level or other changing environmental conditions (Ross et al., 2017). Similarly, the Sa (solar annual) and SSa (solar semi-annual) constituents' periods of approximately 12 and 6 months, respectively, are largely influenced by seasonal weather conditions and storm tracks, leading to high interannual variation; harmonic analysis tests without these two constituents resulted in large discontinuities between adjacent years.

Over each tidal cycle, the maximum of the observed TWL peaks between the High/Low and hourly time series was aligned with predicted tide peaks within +/- 3 hours of each other. The time offset was extended to +/- 6 hours if no High/Low or TWL peaks were found within +/- 3 hours (this was required for < 100 tidal peaks across all gauges over the study time period, and occurred only for gauges within the Chesapeake Bay). Total resultant count was 28,231 tidal peaks per gauge for 1980-2019. The difference between the maximum observed TWL and maximum predicted tide level over each tidal cycle was computed as skew surge.

Daily Weather Maps provided by the NOAA Central Library Data Imaging Project (Ritterbush, 2012) were reviewed alongside observed water levels during the approach to Delmarva of each of the

144 TCs. A time window was manually identified that encapsulated each TC's likely direct influence on water levels within our study region. It often occurred that winds from surface high pressure systems and/or mid-latitude cyclones and associated fronts were influencing water levels in one or both of the bays coincidentally with the approach of the TC. In cases where a suitable time window without other significant weather systems could not be identified, the TC was removed from further analysis. TCs that seemed to have little to no effect on water levels (e.g., they were far away form Delmarva) were left in the analysis provided that no other weather system was significantly impacting the study region at that time, resulting in a near-zero (slightly positive or negative) skew surge for some storms. This manual method of determining a TC-caused flood event was preferred to automated techniques that track low-pressure centers from model reanalyses (Colle et al, 2010; Booth et al, 2016) because of its flexibility in accounting for both high and low pressure systems (regardless of distance to the TC), passing cold fronts, other potential weather scenarios, and places more weight on surface station observations. Although there is potential for false-positive errors (i.e., removing a TC that should remain), this method provides a more conservative approach to assessing surge levels and spatial variability specifically attributed to tropical cyclones.

Median time window was 24 hours before and 18 hours after the TC's closest approach to Delmarva, although in rare cases the window was extended to several days. Ultimately, 38 TCs were removed from the analysis, leaving a total of 106, approximately 2.6 per year on average. For the remainder of this study, this subset of storms will be referred to as Delmarva TCs. Maximum skew surge and maximum TWL ("storm tide") at all tidal peaks occurring within each Delmarva TC's time window were extracted. Storm tides and skew surges were detrended about the mean and normalized by the standard deviation over all 1980 – 2019 tidal peaks at each gauge independently. The detrended, normalized storm tide and skew surge are referred to as the storm tide index (STI) and skew surge index (SSI), respectively.

Distributions of skew surge and SSI values from TCs were computed at each tide gauge over all Delmarva TCs (N = 106). SSI was then compared to STI for each storm using Spearman Rank correlation. Spearman Rank correlation, a non-parametric method, was chosen over the Pearson Product-Moment method to compute correlations considering TC-caused skew surges (as well as storm tides and the normalized, detrended indexes) do not follow a Normal distribution (refer to section 3.1). Correlations were computed for skew surge against maximum NTR for each storm. Skew surge instead of SSI was chosen for this comparison as the NTR time series was not detrended or normalized.

SSI was also compared to the distance of each Delmarva TC's closest approach to the Delmarva Peninsula, regardless of the storm's track direction of movement. Influence of distance on storm surge is compounded by storm size, strength of winds, direction of winds, direction of storm movement, and the location of the tide gauge relative to the storm's direction (e.g., the right or left front quadrant of the TC). The only storm-specific characteristic used in the current study is the location of the TC storm track, and many of the other relevant characteristics are not available in IBTrACS for the full 40-yr time period (most only since 2004). It is not the intent of this study to determine which of these variables are most important to storm surge. However, the distance away of the storm track is often cited and frequently used in storm preparation and awareness campaigns.

2.5 Regional Skew Surge

Since each gauge location has unique tidal characteristics (e.g., mean sea level, tidal range), the STI and SSI derived for each Delmarva TC were averaged over all gauges within each bay. The gauges at Atlantic City and Wachapreague were included with Delaware Bay and Chesapeake Bay, respectively, as listed in Table 1. This allowed for a distinct measure of TC-based water levels per bay for each storm with equal relative weights across gauges. Missing data were ignored in the averaging as no storm had more than one gauge with missing information.

To investigate sub-bay regional variability, cross-correlations and Principal Components Analysis (PCA) were performed on the STI and SSI to identify tide gauges with similar responses. Cross-correlations were computed using Spearman Rank coefficient. PCA with variable clustering was also run on the STI and SSI to aid in grouping of gauges into like regions. STI and SSI for each storm were then averaged across gauges that lie within the identified sub-bay geographic regions. Distributions and cross-correlations among regions were also computed. Each Delmarva TC was then ranked based on mean SSI for each bay and sub-bay region. Storms that were highly ranked in one region/bay as opposed to the others were noted.

Additionally, K-Means clustering was run on the Delmarva TC spatial pattern of SSI across all 12 tide gauges, from upper Delaware Bay to lower Chesapeake Bay. The spatial pattern of SSI is termed the "surge profile" of the storm. JMP Pro 15 statistical software was used to perform the clustering. K-Means is an unsupervised clustering technique that aggregates vectors of data (in our case, each storm's 12 data points of SSI at each gauge) into common sets based on each vector's (i.e., storm's) distance to a set number (K) of means in each dimension. The mean of each dimension is moved upon each pass of the algorithm to minimize the cumulative distance of each vector to its cluster mean. Although K-Means is sensitive to the sort order of the input data, several tests of different sort orders resulted in very similar clustering of storms. The cubic clustering criterion score was used to determine the optimum number of clusters. To determine if a storm's surge profile is associated with the location of its track though the Delmarva region, storm tracks were plotted for all storms within each K-Means cluster. A qualitative (rather than quantitative) assessment was performed on the storm's track position relative to the surge profile.

3 Results

3.1 Delmarva Tropical Cyclone Storm Tide and Skew Surge Summary

Mean storm tides over all Delmarva TCs (Table 2) range from a minimum of 0.48 m at ANN to a maximum of 1.36 m at PHL. Higher storm tides are observed in the Delaware Bay than in the Chesapeake Bay as well as in upper bays compared to the lower bays. This geographic pattern in storm tides nearly identically ($r = 0.99$) matches the pattern of the MHHW tidal datum currently published by NOAA. After detrending and normalization, the relationship of STI to MHHW flips to a strong negative relationship ($r = -0.61$). Largest STI values are in the Chesapeake over the Delaware Bay, and in the lower bays over the upper bays. PHL and RDY have the highest mean storm tides but lowest mean STI. Relationship of storm tides to MSL is similar as to MHHW albeit weaker ($r = -0.39$).

Table 2. *Mean and standard deviation of storm tide and skew surge of Delmarva tropical cyclones, 1980 – 2019. Storm tides and tidal datums referenced to NAVD88 meters. Mean Seal Level (MSL) and Mean Higher-High Water (MHHW) tidal datums defined by NOAA for the current National Tidal Datum Epoch (NTDE) 1983-2001. STI/SSI = storm tide/skew surge index (detrended and normalized versions of storm tide/skew surge based on full study time period.)*

Station		Storm Tide		STI		Skew Surge		SSI		Tidal Datum	
	N	Mean	SD	Mean	SD	Mean	SD	Mean	SD	MSL	MHHW
Philadelphia	106	1.36	0.23	1.30	0.84	0.22	0.23	1.12	1.25	1.09	0.12
Reedy Point	105	1.12	0.19	1.26	0.76	0.18	0.20	1.04	1.16	0.99	-0.02
Lewes	105	0.90	0.27	1.45	1.07	0.24	0.27	1.48	1.75	0.62	-0.12
Cape May	106	1.00	0.25	1.37	0.96	0.22	0.24	1.40	1.60	0.74	-0.14
Atlantic City	106	0.86	0.27	1.32	1.05	0.22	0.27	1.31	1.74	0.61	-0.12
Baltimore	106	0.52	0.26	1.40	1.12	0.21	0.27	1.17	1.49	0.25	-0.01
Annapolis	106	0.48	0.24	1.46	1.13	0.20	0.24	1.20	1.45	0.20	-0.02
Cambridge	106	0.54	0.21	1.44	1.04	0.19	0.21	1.22	1.33	0.29	-0.03
Lewisetta	106	0.51	0.24	1.58	1.24	0.20	0.22	1.38	1.51	0.21	-0.02
Kiptopeke	104	0.62	0.27	1.75	1.40	0.24	0.26	1.71	1.93	0.32	-0.15
Sewells Point	106	0.71	0.33	1.82	1.65	0.28	0.32	1.80	2.15	0.35	-0.08
Wachapreague	97	0.86	0.30	1.54	1.30	0.26	0.27	1.54	1.77	0.57	-0.11

Mean skew surges are more consistent geographically than storm tides, showing very little change across the study region, although the standard deviations and range are similar to storm tides at only 1/2 to 1/6 of the magnitude of the mean. Higher mean skew surges are toward the extreme upper and lower ends and smaller means towards the middle of each bay, ranging from a minimum of 0.18 m at RDY to a maximum of 0.28 m at SEW. Mean skew surges show very little relationship to MHHW and a negative relationship to MSL ($r = -0.42$). After detrending and normalization, the relationship of SSI to MHHW and MSL stayed negative but strengthened ($r = -0.35$ and -0.67, respectively). Larger mean SSI values are found in the lower bays over the upper bays, and in the Chesapeake Bay over the Delaware Bay.

Distribution of skew surge for the Delmarva TCs do not follow a Normal distribution, confirmed by Anderson-Darling test statistic (Figure 4). Shape of the distributions show the typical characteristics of upper tail (extreme values) portion of a normally distributed population, asymmetric right-skewed with a greater number of outliers on the upper end than the lower end. Storm tide distributions (Supplementary Figure 3) are more evenly distributed but still show a skewed upper end tail. (Box plots of these distributions are shown in Supplementary Figure 4.) Many studies have shown extreme high coastal flood levels from tide gauges follow similar extreme value distributions (Tebaldi et al., 2012; Sweet et al., 2014; USACE 2014; Marcos et al., 2015; Moftakhari et al., 2015; Booth et al., 2016; Rashid et al., 2019). The larger population of tidal peak maximum TWL and skew surge (1980-2019, N = 28,231) from which the Delmarva TC-based storm tides and skew surges were extracted, did indeed closely follow the Normal distribution over the long-term once detrended. The steepest curves (i.e., highest probability of smaller surges) occur in the upper bays except for the most north gauges in each bay, namely PHL and BAL, The detrended and normalized STI and SSI distributions for each gauge (not shown) hold essentially the same characteristics except with the expected shifted means and deviations.

SSI exhibits a strong, positive relationship to STI at all tide gauges (Figure 5). The detrending and standardization allows for a more direct comparison of the relative influence of each storm.

Correlations are consistent among sites within each bay, with Delaware Bay at 0.70 – 0.76 and Chesapeake Bay showing higher correlations at 0.82 – 0.89. Sites in the lower bays demonstrate slightly more scatter than in the upper bay, although correlations at all sites are statistically significant at the $p = 0.01$ level. The amount of scatter represents the number of storms with larger relative differences between storm-produced surge and total water level. Hurricane Isabel 2003 is the extreme event in the upper Chesapeake Bay as it produced significantly larger skew surge and storm tide than other storms.

Similarly, skew surge exhibits a strong, positive relationship to maximum NTR (Figure 6). Correlations at all sites are statistically significant at the $p = 0.01$ level. The diagonal dashed line represents one-to-one ratio. Deviations from this line denote storm events when maximum residual occurred at tidal phases other than at tidal peaks. Largest differences occur during the largest skew surge events at the upper Delaware Bay sites, which also have the lowest correlations and relatively broad scatter, even at low surge levels. Over a single tidal cycle, skew surge must be equal to or less than maximum NTR, by definition, however during a storm event that covers multiple tidal cycles, this does not necessarily need to be the case. In our analysis, across all storms and gauges, skew surge was greater than maximum NTR by more than 1 cm only about 25 times, with a maximum difference of approximately 4 cm.

An inverse relationship is evident between SSI and distance to TC closest approach, with correlations ranging from $r = -0.26$ at SEW to $r = -0.37$ at both LEW and CAP (Supplementary Figure 5). Highest correlations are in lower Delaware Bay and lowest correlations in the lower Chesapeake Bay. Although correlations are statistically significant at $p = 0.01$ level, there is broad scatter and similar SSI amounts (especially at lower surge levels) were produced by storms from nearly all distances.

3.2 Sub-bay Regionalization

Cross-correlations on SSI and STI produced from Delmarva TCs across all 12 tide gauges showed strong regional relationships (Figure 7 and Supplementary Tables 1 and 2). Natural groupings of gauges of $r = 0.88$ and above (red regions in Figure 7) emerge within the same geographic regions. Strong distinctions can be noted between gauges in the upper bay and lower bay regions. PCA with variable clustering was run on the SSI and STI (results not shown) and supported results from the cross-correlation analysis. Results indicate regions as: Upper Delaware Bay (PHL, RDY), Lower Delaware Bay (LEW, CAP, ATL), Upper Chesapeake Bay (BAL, ANN, CAM), and Lower Chesapeake Bay (KIP, SEW, WAC). Observations at LWS showed similar correlations with gauges in both the upper and lower Chesapeake Bay regions and had the lowest correlations with gauges in its immediate vicinity. Hence, LWS was not assigned to any sub-bay region. Cross-correlations run on long-term daily maximum skew surge and TWL for 1980-2019 (results not shown) support the same geographic regions. Although not in the same geographic region, LEW correlates highly with gauges in the lower Chesapeake Bay, while WAC correlates highly with gauges in the lower Delaware Bay.

SSI values were averaged across each of the sub-bay regions for each Delmarva TC. The Chesapeake Bay regions have higher mean SSI values than the corresponding Delaware Bay regions, and the lower bay regions have higher mean SSI than upper bay regions. Most notably, the lower bay regions have higher correlations to each other than to their respective upper bay regions, and likewise for the upper bay regions. Relationship between the Upper and Lower Chesapeake regions show the lowest correlation of any pair of groups ($r = 0.50$).

Table 3. *Means and cross-correlations of skew surge index (SSI) across Delmarva tropical cyclones, 1980 – 2019. All correlations statistically significant at p = 0.01 level.*

Region	Mean SSI	Cross-Correlation of SSI			
		Delaware Bay Upper	Delaware Bay Lower	Chesapeake Bay Upper	Chesapeake Bay Lower
Upper Delaware	1.08	1.00	0.68	0.79	0.59
Lower Delaware	1.39	0.68	1.00	0.56	0.88
Upper Chesapeake	1.19	0.79	0.56	1.00	0.49
Lower Chesapeake	1.70	0.59	0.88	0.49	1.00

Distributions of regional SSI (Supplementary Figure 6), do not follow a Normal distribution, confirmed by Anderson-Darling statistic, but are more closely related to extreme value distributions similar to distributions of tide gauges. Upper bays experience a steeper, more uniform decline than lower bays, although all regions include outlier storms in the far upper end. Additionally, regional SSI against STI showed similar behavior as tide gauge analysis. Most of the deviations occur at the lower SSI values and the upper bays have slightly more scatter than lower bays. Chesapeake Bay shows higher correlations of SSI to STI (r = 0.86 in both upper and lower Bay regions) than does Delaware Bay (r = 0.73 and 0.72 for the upper and lower Bay regions, respectively).

3.3 Top Surges of Delmarva Tropical Cyclones

SSI was averaged over all gauges within each bay boundary (i.e., LWS was included for the Chesapeake Bay; ATL and WAC were not included for either Bay) for each Delmarva TC (Figure 8). As noted earlier, large variations exist although most storms have smaller SSI values under 2. Larger surge events are typically 2 to 7. Mean SSI across all storms are 1.31 and 1.42 for the Delaware and Chesapeake Bays, respectively. Although many storms have similar SSI for each bay, especially for the smaller surge events, some stand out for their differences. Hurricanes Isabel (2003) and Fran (1996) impacted the Chesapeake more than the Delaware Bay by the largest margin, whereas likewise, Hurricanes Gloria (1985) and Sandy (2012) impacted the Delaware more than the Chesapeake Bay. The top 10 Delmarva TCs with the largest differences in SSI are listed in Supplementary Table 3.

The top 25 Delmarva TCs were ranked by SSI in each bay (Table 4). The year and month represent the time of the storm's closest approach, the great majority occurring in September and October. Status column represents the most common value of the IBTrACS USA_STATUS attribute while the storm was present within the 750 km buffer around Delmarva, including times before and after the storm's closest approach. Both bays have many top storms in common, notably Hurricanes Sandy (2012), Isabel (2003), and Not Named (1991), claiming 3 of the top 5 spots in each bay.

Delmarva TCs also show significant sub-bay regional differences. Supplementary Tables 4 and 5 list the top 25 Delmarva TCs ranked separately for each of the four sub-bay regions. Surprisingly, Hurricane Isabel (2003) was the top ranked storm for the Upper Delaware Bay although it is typically known as a Chesapeake Bay flood event. Hurricanes Hugo (1989), Fran (1996), and Hanna (2008) produced higher surges in upper bays than lower bay regions (Supplementary Figure 8), whereas Hurricane Gloria (1985), Not Named (1991), and Hurricane Irene (2011) produced higher surges in the lower bay regions. (Note that Not Named (1991) may be better known as the Halloween Blizzard of 1991 or The Perfect Storm of 1991.)

Table 4. *Top 25* Delmarva tropical cyclones*, ranked by skew surge index (SSI), for the Delaware and Chesapeake Bay, 1980 – 2019. Year and Month note the time of storm's closest approach to Delmarva. Status represents the most common value of USA_STATUS attribute in the IBTrACS database while the storm is within the 750 km buffer. EX = Extratropical, HU = Hurricane, TS = Tropical Storm, TD = Tropical Depression, SS = Subtropical Storm, DB = Disturbance. Refer to the IBTrACS Version 4 Technical Documentation for more details.*

	Delaware Bay					**Chesapeake Bay**			
Rank	**Name**	**Year**	**Month**	**Status**		**Name**	**Year**	**Month**	**Status**
1	SANDY	2012	10	EX		ISABEL	2003	9	HU
2	GLORIA	1985	9	HU		SANDY	2012	10	EX
3	NOT_NAMED	1991	10	EX		ERNESTO	2006	9	EX
4	WILMA	2005	10	HU		NOT_NAMED	1991	10	EX
5	ISABEL	2003	9	HU		FRAN	1996	9	TD
6	ERNESTO	2006	9	EX		WILMA	2005	10	HU
7	IRENE	2011	8	HU		MELISSA	2019	10	EX
8	FLOYD	1999	9	HU		DENNIS	1999	9	TS
9	MELISSA	2019	10	EX		IRENE	2011	8	HU
10	DANIELLE	1992	9	TS		NOT_NAMED	1981	11	SS
11	NOT_NAMED	1981	11	SS		FLOYD	1999	9	HU
12	JOSEPHINE	1996	10	EX		DORIAN	2019	9	HU
13	NOT_NAMED	2005	10	EX		DANIELLE	1992	9	TS
14	JOSEPHINE	1984	10	HU		HERMINE	2016	9	EX
15	BERTHA	1996	7	TS		JOSEPHINE	1984	10	HU
16	NOEL	2007	11	EX		JOSE	2017	9	TS
17	DEAN	1983	9	TS		GORDON	1994	11	HU
18	JOSE	2017	9	TS		BONNIE	1998	8	HU
19	KYLE	2002	10	TS		GLORIA	1985	9	HU
20	HERMINE	2016	9	EX		DEAN	1983	9	TS
21	DENNIS	1999	9	TS		JOSEPHINE	1996	10	EX
22	EDOUARD	1996	9	HU		HUGO	1989	9	HU
23	DENNIS	1981	8	TS		FLORENCE	2018	9	HU
24	BARRY	2007	6	EX		HANNA	2008	9	TS
25	HANNA	2008	9	TS		CHARLEY	1986	8	TS

3.4 Spatial Patterns of Skew Surge

Analogous to grouping tide gauges based on their cross-correlations of SSI, the Delmarva TCs were grouped using K-Means clustering algorithm based on their spatial pattern and magnitude of SSI (i.e., surge profile) throughout the study region. Only Delmarva TCs with valid surge data at all 12 tide gauges (N = 93) were used as input to the clustering algorithm. Clusters of 3 to 15 were tested with 13 clusters ultimately chosen based on the cubic clustering criterion score. Each resultant cluster of storms represent a unique combination of magnitude and pattern of variability of SSI. Several of these clusters had very few storms, particularly storms with the largest skew surges, and were grouped with other clusters with similar surge profiles into cluster groups. Surge profile plots of storms within each cluster are shown in Figure 9A-F and the associated storm tracks are mapped in Figure 10A-F. Individual clusters in the profile plots and storm track maps are denoted by different colors.

Cluster Group 1 is composed of two individual clusters representing storms with the lowest overall surge magnitude, with SSI generally less than 2, and little variation across gauges (Figures 9A and 10A). Group 1 contains the most storms of any cluster group by far, with the difference between the individual clusters being differences in the pattern of upper vs lower bays (i.e., they are out of phase with each other). Tracks for these clusters are quite varied in their origination location and distance to Delmarva, yet nearly all pass to the southeast. Group 2 (Figures 9B and 10B) surge profiles are also approximately evenly distributed albeit with consistently larger SSI. Tracks in Group 2 are generally close together passing almost directly over Delmarva. Group 3 (Figures 9C and 10C) is composed of two individual clusters that are similar to Group 2 in SSI magnitude but start to have a more pronounced spatial variation than previous clusters, with higher SSI in the lower bay than upper bay regions and a slight emphasis on the Chesapeake Bay. Tracks in Group 3 are generally farther offshore to the southeast, except for two storms (Dennis (199) and Florence (2018)) that track to the west of Delmarva. Both of these storms had close approaches to Delmarva from the south/southeast before changing direction to the west/northwest.

Group 4 (Figures 9D and 10D) also is composed of two individual clusters with very similar spatial variation to Group 3 (i.e., higher SSI in the lower bay than upper bay regions) although larger SSI magnitude across both bays with slight emphasis on the Delaware instead of the Chesapeake Bay. Only three storms make up this group, Hurricanes Sandy (2012) and Wilma (2005) and Not Named (1991). Tracks of these storms were similar and lie further east/northeast than tracks in other clusters (albeit Sandy took a last-minute turn to the west and passed by Delmarva to the north). Group 5 (Figures 9E and 10E) again has the similar spatial pattern as Groups 3 and 4 but the difference between upper and lower bay regions is much larger, with high SSI in one or both of the lower bays, and low SSI in the upper Chesapeake Bay. Three storms make up this group, Hurricanes Gloria (1985), Floyd (1999), and Irene (2011), each of which were assigned to their own individual clusters. All three have nearly identical tracks and similar points of origin (West Caribbean or central Atlantic), passing very close to Delmarva just offshore to the southeast.

The last cluster group, Group 6 (Figures 9F and 10F), is composed of three individual clusters representing the reverse surge spatial pattern from the other clusters. These storms show higher surges in the upper bay than in the lower bay regions, with larger differences than storms in Group 1, and were grouped together based more on similarity of SSI variation than the magnitude. Most of these storms pass to the west of Delmarva. Fran (1996) and Isabel (2003), assigned their own clusters (based on magnitude), have the highest SSI for the upper Chesapeake Bay region, with nearly identical tracks and points of origin.

4 Discussion

The goal of the current study is to quantify the magnitude and regional differences of skew surge in the Delaware and Chesapeake Bays from tropical cyclones rather than the more common flood events due to extra-tropical cyclones (ETCs). Although future increases are projected in the number of major TCs and TC intensification (Kossin et al., 2017), the exact response of ETC cyclogenesis and frequency under global warming is still unclear. TCs make up a significant portion of the top flood events and receive much attention in research activities, emergency preparation action, and public awareness campaigns. Our focus was not to examine the storm-specific characteristics (e.g., storm size, atmospheric pressure, wind speed and direction) that contribute to storm surge but rather focus on the net effect of all of these, which is the ultimate metric to use from a risk management perspective.

Since skew surge is used in this study rather than maximum NTR, surge values for a particular storm may not match previous reports, such as in NOAA's NHC Tropical Cyclone Reports (NHC, 2020). Maximum NTR can be a reliable indicator of storm surge in areas without significant tide-surge interaction, such as open coastal locations on the US Atlantic Coast (Zhang et al., 2000; Bernier and Thompson, 2007; Mawdsley and Haigh, 2016). This was tested on the Delaware and Chesapeake Bay gauges using Quantile-Quantile (Q-Q) plots and two-sample Anderson-Darling tests. These were run on the NTR during four different tidal phases: High Tide (+/- 1.5 hours from high tidal peak), Falling Tide, Low Tide (+/- 1.5 hours from low tidal peak), and Rising Tide. As examples, Supplementary Figures 1 and 2 show plots for LEW and PHL. None of the gauges in our study appear to exhibit significant tide-surge interaction, in agreement with previous studies.

Closer inspection of the NTR time series did reveal small oscillations at tidal frequencies. Low-pass filters designed to remove these components could be applied to the NTR time series (Shirahata et al., 2016), however, filters can easily decrease amplitude of the signal and care must be taken to not remove water level oscillations (e.g. surge) caused by TCs moving quickly through the region. Additionally, for TCs with durations of multiple tidal cycles, maximum NTR often occurs over low predicted tide, and not indicative of amount of flooding over the next (or previous) high tide. Hence, maximum NTR is dependent upon numerous factors, and perhaps not as reliable (Balstone et al., 2013) or useful (Williams et al., 2016) an estimate of meteorological component of increased sea level as skew surge.

Figure 6 shows very high correlation coefficients between skew surge and max NTR for Delmarva TCs. High correlations values indicate how well skew surge and max NTR are linearly related, not necessarily how close they are in magnitude. Across all gauges and Delmarva TCs, maximum NTR is greater than skew surge by 10 cm or more for 29% of events, and by 20 cm or more for 11.5% of events, most prominently at the upper Delaware Bay sites. This difference in timing could be indicative of tide-surge interactions or other phenomena occurring in this region but is beyond the scope of this paper. Large differences at large surge levels can lead to misinterpretation and potential overestimation of the amount of flooding from major, usually well-publicized, storms.

Due to the geomorphology and bathymetry of the region, tides are higher and exhibit wider range in the upper Delaware Bay than in other regions. Delmarva TC storm tides in the upper Delaware Bay were accordingly the highest in the study region (Table 2). Interaction of tides and surge, in addition to spatially variable relative sea-level rise, are complex yet play a large role in the amount coastal flooding a location observes. Detrending and normalizing storm tides and skew surges removes this influence, allowing for a better comparison of gauges over space and of storms over time. Gauges in the upper Delaware Bay resulted in the lowest STI, meaning that the relative coastal flooding due to TCs is least in the upper Delaware Bay and most in the lower Chesapeake Bay. Likewise, STI shows a strong negative correlation to MHHW, decreasing relative influence of TC flooding in areas of higher tides.

The same concept holds true for storm surge. Results in Tables 2 and 3 show that the Chesapeake Bay regions experience higher relative surges from TCs than the Delaware Bay. Likewise, the lower bays experience higher relative surges from TCs than do the upper bays. Relative influence of TC surge is expected to increase towards the south and east. TCs that stay just offshore, keeping Delmarva sites in the front left quadrant, bring strong southeast and east winds as they travel north/northeast direction, pushing water directly on the ocean coast an into the bays. As they pass, northwest winds that parallel the coast induce Ekman transport into the bays, at times competing against the local winds, increasing the surface water levels in the lower bays more than upper bays

(Garvine 1985). Differences in surge among TCs depend on duration, size, and strength of wind field.

Cross-correlations (Figure 7) and PCA on SSI demonstrate sub-bay regional differences. LWS has similar correlations to gauges in both the lower and upper Chesapeake Bay regions but not as strong as among gauges within those regions. Generally, surge at LWS tended to follow the behaviour of lower bay gauges during TCs that were east of Delmarva and of upper bay gauges during TCs that were west of Delmarva, although the magnitude was usually somewhere between. The central location of LWS makes it valuable for assessing surge in the Chesapeake Bay albeit problematic if assigned to either an upper or lower bay region.

Table 3 shows that lower regions in each bay respond to TCs more similarly to each other than to their respective upper regions. The distance between the bay inlets is relatively small compared to the size of the TC and their tracks, and drivers such as wind direction or Ekman transport would impact these areas similarly. This may run counter to public perception since many outreach and planning activities tend to focus on The Delaware and Chesapeake Bays separately. The Bays fall into separate NWS Forecast Offices, who are responsible for sending out real-time weather and coastal flood advisories and have separate state initiatives and SLR planning committees (Boesch et al., 2018; Callahan et al., 2017). This is understandable considering the funding sources and political directives, however, perhaps the results of this study show that regions of each bay could be addressed collectively regarding surge risk hazards.

The World Meteorological Organization states that hurricanes are named to help with "disaster risk awareness, preparedness, management, and reduction," and names are retired "due to sensitivity" from the destruction they cause (WMO, 2020). Ranking of storms can be looked upon in a similar vein by meteorologists and emergency managers, recalling local knowledge from pervious experiences to help in outreach. As well, it could provide scientists and planners analog storms with similar surge potential to compare against. Separate ranking by geographic region helps focus preparedness efforts.

Highly ranked storms in both bays include Hurricanes Isabel (2003), Wilma (2005), Ernesto (2006), Sandy (2012), and Not Named (1991). All of these were very large, strong storms with wide reaching wind fields that transitioned to extratropical near Delmarva. The high wind speeds and longer duration of swell directed at Delmarva contributed to the extreme surge levels from these storms. Surge from Isabel (2003) was an extreme outlier in the Chesapeake Bay compared to the other TCs primary due to its linear track, traveling southeast to northwest while keeping the Chesapeake in its right-front quadrant, continually pushing water up the bay (NHC, 2014). Gloria (1985) would be Isabel's counterpart for the Delaware Bay, although its fast speed and track to the east of Delmarva limited its most severe impacts to the lower bay region.

Although many factors influence storm surge, distance and position of storm track do play a significant role. Statistically significant correlations were found between SSI and the minimum distance to Delmarva by each TC (Supplementary Figure 5). Clustering analysis shows, at least qualitatively, a relationship exists between spatial variability of surge in the bays to storm track. In both analyses, distance alone is not a strong predictor of surge as small surges can occur at short distances and a wide variety of tracks (Figure 10A). Cluster Group 3 shows the typical pattern of moderate levels if surge with larger values in lower bays and smaller values in the upper bays. Nearly all of these stayed just offshore to the east. The two TCs in this group that passed to the west of Delmarva, Dennis (1992) and Florence (2018), had unique tracks in that they approached from the south impacting water levels near Delmarva, before turning west and eventually northward, spending long durations within the 750 km buffer.

Tracks for the three storms in Cluster Group 5 (Gloria (1985), Floyd (1999), and Irene (2011)), travelled directly over Delmarva in a south to north direction and caused high surge values and large variations between upper and lower bays (Figure 10E). TCs that impacted the lower bays more than the upper bays tended to track parallel to the coast east of Delmarva (Figures 10C-E). TCs that impacted the upper bays more than lower bays tended to stay to the west of Delmarva (Figure 10F). Nearly all of these storm tracks in Cluster Group 6 pass to the west of Delmarva on a northerly track, allowing stronger winds on the right side of the cyclone to impact the region for longer durations. Many of these TCs also originated in the Atlantic Ocean and had longer lifetimes.

In order to generalize some of the conclusions in this paper, a similar methodology could be applied to extratropical flood events at the same tide gauge locations. As well, a more thorough statistical analysis of surge profiles compared to specific TC meteorological characteristics would quantify the relative contributions of the major drivers of TC-caused surge in the Delaware and Chesapeake Bays. Tropical cyclones, like all coastal storms, are multi-hazard weather events, with storm surge the most destructive and lethal hazard. In a changing environment, there continues to be a need to improve storm surge forecasting and implement strategies to minimize the damage of coastal flooding (CCPR 2016; Rahmstorf, 2017; Chippy and Jawahar, 2018). Results from this analysis can provide insight on the potential regional impacts of coastal flooding from tropical cyclones in the Mid-Atlantic region.

Abbreviations

NOAA Tide Gauge Locations – Philadelphia (PHL), Reedy Point (RDY), Lewes (LEW), Cape May (CAP), Atlantic City (ATL), Baltimore (BAL), Annapolis (ANN), Cambridge (CAM), Lewisetta (LWS), Kiptopeke (KIP), Sewells Point (SEW), Wachapreague (WAC)

CO-OPS - NOAA Center for Operational Oceanographic Products and Services

DEMA - Delaware Emergency Management Agency

ETC - Extratropical Cyclone (sometimes called mid-latitude cyclones)

FEMA - Federal Emergency Management Agency

HURDAT2 - Atlantic Hurricane Database (HURDAT2)

IBTrACS - International Best Track Archive for Climate Stewardship

MHHW - Mean Higher-High Water tidal datum

MSL - Mean Sea Level tidal datum

NAVD88 - North American Vertical Datum 1988

NCEI - NOAA National Centers for Environmental Information

NHC – NOAA National Hurricane Center (division of the National Weather Service)

NOAA - National Oceanic and Atmospheric Administration

NOS – NOAA National Ocean Service

NTDE - National Tidal Datum Epoch

NTR - Non-tidal residual

NWLON - NOAA NOS National Water Level Observation Network

PORTS - NOAA National Ocean Service Physical Oceanographic Real-Time System

SSI - Storm Surge Index

SST - Sea Surface Temperature

STI - Storm Tide Index

SURGEDAT - A database specifically designed to store storm surge data with 700 tropical surge events around the world and more than 8,000 unique tropical high water marks along the U.S. Gulf and Atlantic Coasts since 1880

TC - Tropical Cyclone

TWL - Total water level

USACE - US Army Corps of Engineers

WMO - World Meteorological Organization

References

Batstone, C., Lawless, M., Tawn, J., Horsburgh, K., Blackman, D., McMillan, A., D. Worth, Laeger, S., and Hunt, T. (2013). A UK best-practice approach for extreme sea-level analysis along complex topographic coastlines. *Ocean Engineering*, 71, 28–39. doi:10.1016/j.oceaneng.2013.02.003.

Bernhardt, J. E., and DeGaetano, A.T. (2012). Meteorological factors affecting the speed of movement and related impacts of extratropical cyclones along the U.S. east coast. *Natural Hazards*, 61, 1463–1472. doi:10.1007/s11069-011-0078-0

Bernier, N. B. and Thompson, K. R. (2007). Tide-surge interaction off the east coast of Canada and northeastern United States. *Journal of Geophysical Research*, 112, C06008. doi:10.1029/2006JC003793

Blake, E. S. and Gibney, E. J. (2011). The deadliest, costliest, and most intense United States tropical cyclones from 1851to 2010 (and other frequently requested hurricane facts). NOAA Technical Memorandum NWS NHC-6. 49 pp.

Boon, John D., Mitchell, M., Loftis, J. D., and Malmquist, D. L. (2018). Anthropogenic Sea Level Change: A History of Recent Trends Observed in the U.S. East, Gulf and West Coast Regions, Special Report No. 467 in Applied Marine Science and Ocean Engineering, prepared by Virginia Institute of Marine Science, VA, 76 pp.

Booth, J. F., Rider, H. E., and Kushnir, Y. (2016). Comparing hurricane and extratropical storm surge for the Mid-Atlantic and Northeast Coast of the United States for 1979–2013. *Environmental Research Letters*, 11:9, 094004. doi:10.1088/1748-9326/11/9/094004

Boesch, D. F., Boicourt, W.C., Cullather, R.I., Ezer, T., Galloway, G.E., Jr., Johnson, Z.P., Kilbourne, K.H., Kirwan, M.L., Kopp, R.E., Land, S., Li, M., Nardin, W., Sommerfield, C.K., Sweet, W.V. (2018). Sea-level Rise: Projections for Maryland 2018, 27 pp. University of Maryland Center for Environmental Science, Cambridge, MD.

[CCPR] Council on Climate Preparedness and Resilience. (2016). Opportunities to Enhance the Nation’s Resilience to Climate Change. 46 pp.

Callahan, J. A., Horton, B.P., Nikitina, D.L., Sommerfield, C.K., McKenna, T.E., and Swallow, D. (2017). Recommendation of Sea-Level Rise Planning Scenarios for Delaware: Technical Report, prepared for Delaware Department of Natural Resources and Environmental Control (DNREC) Delaware Coastal Programs. 116 pp.

Chesapeake Bay Program. (2020). State of the Chesapeake. https://www.chesapeakebay.net/state [Accessed August 18, 2020].

Chippy, M. R., and Jawahar, S. S. (2018). Storm Surge and its Effect-A Review on Disaster Management in Coastal Areas. *Civil Engineering Research Journal*, 4, 5, 555649. doi:10.19080/CERJ.2018.04.555649

Codiga, D.L. (2011). Unified Tidal Analysis and Prediction Using the UTide Matlab Functions. Graduate School of Oceanography, University of Rhode Island, GSO Technical Report 2011-01, 60 pp.

Colle, B. A., Rojowsky, K., and Buonaito, F. (2010). New York City Storm Surges: Climatology and an Analysis of the Wind and Cyclone Evolution. *Journal of Applied Meteorology and Climatology*, 49, 85-100.

Colle, B. A., Booth, J. F., and Chang, E. K. M. (2015). A Review of Historical and Future Changes of Extratropical Cyclones and Associated Impacts along the US East Coast. *Current Climate Change Reports*, 1, 3, 125-143. doi:10.1007/s40641-015-0013-7

[COOPS] NOAA National Ocean Service Center for Operational Oceanographic Products and Services. (2020a). Sea Level Trends. https://tidesandcurrents.noaa.gov/sltrends/ [Accessed August 18, 2020].

[COOPS] NOAA National Ocean Service Center for Operational Oceanographic Products and Services. (2020b). API for Data Retrieval. https://api.tidesandcurrents.noaa.gov/api/prod/ [Accessed April 9, 2020].

[COOPS] NOAA National Ocean Service Center for Operational Oceanographic Products and Services. (2020c). NOAA Tide Predictions. https://tidesandcurrents.noaa.gov/tide_predictions.html [Accessed April 9, 2020].

[DEMA] Delaware Emergency Management Agency (2018). State of Delaware All-Hazard Mitigation Plan. 308 pp.

Dolan, R. and Davis, W. E. (1992). An intensity scale for Atlantic coast Northeast storms. Journal of Coastal research, 8, 4, 840 – 853.

Eagleson, P. S., and Ippen, A. T. (1966). Estuary and coastline hydrodynamics. New York, McGraw-Hill Book Co.

Ellis, J. T., and Sherman, D. J. (2015). Perspectives on Coastal and Marine Hazards and Disasters, in Coastal Marine Hazards, Risks, and Disasters [John F. Shroder, Jean T. Ellis, and Douglas J. Sherman, eds]. doi:10.1016/B978-0-12-396483-0.01001-3

Elsner, J.B., and Kara, A. B. (1999). Hurricanes of the North Atlantic: Climate and Society. Oxford University Press, New York.

[FEMA] Federal Emergency Management Agency (2013). Region III: Coastal Analysis and Mapping. (2013). Region 3 Storm Surge Study. https://sites.google.com/site/r3coastal/home/storm-surge-study [Accessed April 9, 2020].

Harris, D. L. (1991). Reproducibility of the harmonic constants. Tidal Hydrodynamics, in B. P. Parker, Ed., John Wiley and Sons, 753–771.

Harleman, D. R. F. (1966). Real Estuaries, in Estuary and Coastline Hydrodynamics, In: Ippen, A.T., ed. (McGraw-Hill, New York) 522–545.

Hirsch, M. E., A. T. Degaetano, and S. J. Colucci (2001). An East Coast Winter Storm Climatology. *Journal of Climate*, 14, 882-899. doi:10.1175/1520-0442(2001)014<0882:AECWSC>2.0.CO;2

Holgate, S. J., Matthews, A., Woodworth, P. L., Rickards, L. J., Tamisiea, M. E., Bradshaw, E., Foden, P. R., Gordon, K. M., Jevrejeva, S., and Pugh, J. (2013). New Data Systems and Products at the Permanent Service for Mean Sea Level. *Journal of Coastal Research*, 29, 3, 493 – 504. doi:10.2112/JCOASTRES-D-12-00175.1

Jay, A., D.R. Reidmiller, C.W. Avery, D. Barrie, B.J. DeAngelo, A. Dave, M. Dzaugis, M. Kolian, K.L.M. Lewis, K. Reeves, and D. Winner (2018). Overview. In Impacts, Risks, and Adaptation in the United States: Fourth National Climate Assessment, Volume II [Reidmiller, D.R., C.W. Avery, D.R. Easterling, K.E. Kunkel, K.L.M. Lewis, T.K. Maycock, and B.C. Stewart (eds.)]. U.S. Global Change Research Program, Washington, DC, USA, pp. 33–71. doi: 10.7930/NCA4.2018.CH1

Keim, B., Muller, R., & Stone, G. (2007). Spatiotemporal Patterns and Return Periods of Tropical Storm and Hurricane Strikes from Texas to Maine. *Journal of Climate*, 20:14, 3498-3509.

Knapp, K. R., Kruk, M. C., Levinson, D. H., Diamond, H. J., and Neumann, C. J. (2010). The International Best Track Archive for Climate Stewardship (IBTrACS): Unifying tropical cyclone best track data. *Bulletin of the American Meteorological Society*, 91, 363-376. doi:10.1175/2009BAMS2755.1

Knapp, K. R., Diamond, H. J., Kossin, J. P., Kruk, M. C., and Schreck, C. J. (2018). International Best Track Archive for Climate Stewardship (IBTrACS) Project, Version 4. [North Atlantic Basin since 1980]. NOAA National Centers for Environmental Information. non-government domain https://doi.org/10.25921/82ty-9e16 [Accessed May 18, 2020].

Knutson, T., Camargo, S. J., Chan, J. C. L., Emanuel, K., Ho, C-H., Kossin, James, Mohapatra, M., Satoh, M., Sugi, M., Walsh, K., and Wu, L. (2019). Tropical Cyclones and Climate Change Assessment: Part I: Detection and Attribution. *Bulletin of the American Meteorological Society*, 1987-2007.

Knutson, T., Camargo, S. J., Chan, J. C. L., Emanuel, K., Ho, C-H., Kossin, J., Mohapatra, M., Satoh M., Sugi, M., Walsh, K., and Wu, L. (2020). Tropical Cyclones and Climate Change Assessment: Part II: Projected Response to Anthropogenic Warming. *Bulletin of the American Meteorological Society*, E303-E322. doi:10.1175/BAMS-D-18-0194.1

Kopp, R. E. (2013). Does the mid-Atlantic United States sea level acceleration hot spot reflect ocean dynamic variability? *Geophysical Research Letters*, 40, 3981–3985. doi:10.1002/grl.50781

Kossin, J. P., Hall, T., Knutson, T., Kunkel, K. E., Trapp, R. J., Waliser, D. E., and Wehner, M. F.. (2017). Extreme storms. In: Climate Science Special Report: Fourth National Climate Assessment, Volume I [Wuebbles, D. J., Fahey, D. W., Hibbard, K. A., Dokken, D. J., Stewart, B. C., and Maycock, T. K. (eds.)]. U.S. Global Change Research Program, Washington, DC, USA, pp. 257-276. doi:10.7930/J07S7KXX

Kossin, J. P. (2018). A global slowdown of tropical-cyclone translation speed. *Nature*, 558, 104–107. doi:10.1038/s41586-018-0158-3

Lee., S. B., Li, M., and Zhang, F. (2017). Impact of sea level rise on tidal range in Chesapeake and Delaware Bays. *Journal of Geophysical Research: Oceans*, 122, 3917-3938. doi:10.1002/2016JC012597

Landsea, C. W., and Franklin, J. L. (2013). Atlantic hurricane database uncertainty and presentation of a new database format. *Monthly Weather Review*, 141, 3576-3592.

Leathers, D. J., Kluck, D. R., and Kroczynski, S. (1998). The severe flooding event of January 1996 across North-Central Pennsylvania. *Bulletin of the American Meteorological Society*, 79, 785-797.

Li, M., Zhang, F., Barnes, S., and Wang, X. (2020). Assessing storm surge impacts on coastal inundation due to climate change: case studies of Baltimore and Dorchester County in Maryland. *Natural Hazards*, 103, 2561–2588. doi:10.1007/s11069-020-04096-4

Marcos, M., Calafat, F. M., Berihuete, A., and Dangendorf, S. (2015). Long-term variations in global sea level extremes. *Journal of Geophysical Research: Oceans*, 120, 8115–8134. doi:10.1002/2015JC011173

Mawdsley, R. J., and Haigh, I. D. (2016). Spatial and Temporal Variability and Long-Term Trends in Skew Surges Globally. *Frontiers in Marine Science*, 3, 1-29. doi:10.3389/fmars.2016.00029

McAdie, C. J., Landsea, C. W., Neumann, C. J., David, J. E., Blake, E. S., and Hammer, G. R. (2009). Tropical Cyclones of the North Atlantic Ocean, 1851-2006: With 2007 and 2008 Track Maps Included. National Oceanic and Atmospheric Administration Historical Climatology Series 6-2, 243 pp.

Merrifield, M. A., Genz, A. S., Kontoes, C. P., and Marra, J. J. (2013). Annual maximum water levels from tide gauges: Contributing factors and geographic patterns. *Journal of Geophysical Research: Oceans*, 118, 2535–2546. doi:10.1002/jgrc.20173

Moftakhari, H. R., AghaKouchak, A., Sanders, B. F., Feldman, D. L., Sweet, W., Matthew, R. A., and Luke, A. (2015). Increased nuisance flooding along the coasts of the United States due to sea level rise: Past and future, *Geophysical Research Letters*, 42, 9846–9852. doi:10.1002/2015GL066072

Muller, R. A. and Stone. G. W. (2001). A climatology of tropical storm and hurricane strikes to enhance vulnerability prediction for the Southeast U.S. coast. *Journal of Coastal Research*, 17, 9949-956.

Murakami, H., Delworth, T. L., Cooke, W. F., Zhao, M., Xiang, B., and Hsu, P. C. (2020). Detected climatic change in global distribution of tropical cyclones. *PNAS*, 117:20, 10706-10714. doi:10.1073/pnas.1922500117

[NHC] National Hurricane Center. (2020). NOAA, Tropical Cyclone Reports. https://www.nhc.noaa.gov/data/tcr/ [Accessed May 20, 2020].

[NHC] National Hurricane Center. (2019). NOAA, Storm Surge Overview. https://www.nhc.noaa.gov/surge/ [Accessed January 10, 2019].

[NHC] National Hurricane Center. (2014). NOAA, Tropical Cyclone Report for Hurricane Isabel, 6-19 September 2003. 30 pp.

Needham, H. F., Keim, B. D., and Sathiaraj, D. (2015). A review of tropical cyclone-generated storm surges: Global data sources, observations, and impacts. *Reviews of Geophysics*, 53, 545–591. doi:10.1002/2014RG000477

[NCEI] NOAA National Centers for Environmental Information. (2020). U.S. Billion-Dollar Weather and Climate Disasters. doi:10.25921/stkw-7w73

[NWLON] NOAA National Ocean Service National Water Level Observation Network (NWLON). https://www.tidesandcurrents.noaa.gov/nwlon.html [Accessed August 18, 2020].

Patrick, R. (1994). Rivers of the United States, Volume 1: Estuaries, John Wiley and Sons, 1994. ISBN: 978-0-471-30345-9

[PORTS] NOAA National Ocean Service Physical Oceanographic Real-Time System (PORTS). https://tidesandcurrents.noaa.gov/ports.html [Accessed August 18, 2020].

Pugh, D., and Woodworth, P. (2014). Sea-Level Science: Understanding Tides, Surges, Tsunamis and Mean Sea-Level Changes. Cambridge: Cambridge University Press. doi:10.1017/CBO9781139235778

Rahmstorf, S. (2017). Rising hazard of storm-surge flooding. *PNAS Commentary*, 114, 45, 11806-11808. doi:10.1073/pnas.1715895114

Rappaport, E. (2014). Fatalities in the United States from Atlantic Tropical Cyclones New Data and Interpretation. Bulletin of the American Meteorological Society Insights and Innovations. 341 – 346.

Rashid, M., Wahl, T., Chambers, D., Calafat, F., and Sweet, W. (2019). An extreme sea level indicator for the contiguous United States coastline, *Sci Data*, 6:326, 10.1038/s41597-019-0333-x

Ritterbush, J. (2012). US Daily Weather Maps Project, Reference Reviews, Vol. 26 No. 1, pp. 39-39. doi:10.1108/09504121211195333

Ross, A. C., Najjar, R. G., Li, M., Lee, S. B., Zhang, F., and Liu, W. (2017). Fingerprints of sea level rise on changing tides in the Chesapeake and Delaware Bays. *Journal of Geophysical Research: Oceans*, 122, 8102–8125. https://doi.org/10.1002/2017JC012887

Salehi, M. (2018). Storm Surge and Wave Impact of Low-Probability Hurricanes on the Lower Delaware Bay—Calibration and Application. *Journal of Marine Science and Engineering*, 6, 54.

Sallenger, A. H., K. S. Doran, and P. A. Howd (2012). Hotspot of accelerated sea-level rise on the Atlantic coast of North America. *Nature Climate Change*, 2, 884–888, doi:10.1038/nclimate1597

Sanchez, J. R., G. Kauffman, K. Reavy, A. Homsey. (2012). “Chapter 1.7 - Natural Capital Value” in the Technical Report for the Delaware Estuary and Basin. Partnership for the Delaware Estuary. PDE Report No.17-07 pp. 70-75.

Shirahata, K., Yoshimoto, S., Tsuchihara, T., and Ishida, S. (2016). Digital Filters to Eliminate or Separate Tidal Components in Groundwater Observation Time-Series Data. *Japan Agricultural Research Quarterly*, 50:3, 241-252. doi:10.6090/jarq.50.241

Simpson, R. H. and Lawrence M. (1971). Atlantic hurricane frequencies along the United States coastline. NOAA Tech. Memo. NWS-SR-58, 14 pp.

Smith, A. B, and Katz, R. W. (2013). US billion-dollar weather and climate disasters: data sources, trends, accuracy and biases. *Natural Hazards*, 67, 387-410. Doi:10.1007/s11069-013-0566-5

Spicer, P., Huguenard, K., Ross, L., and Rickard, L. N. (2019). High-frequency tide-surge-river interaction in estuaries: causes and implications for coastal flooding. *Journal of Geophysical Research: Oceans*, 124. Doi:10.1029/2019JC015466

Stephens, S. A., Bell, R. G., and Haigh, I. D. (2020). Spatial and temporal analysis of extreme storm-tide and skew-surge events around the coastline of New Zealand. *Natural Hazards and Earth System Sciences*, 20, 3, 783-796.

Strobach, E, Sparling, L. C., Rabenhorst, S. D., and Demoz, B. (2018). Impact of Inland Terrain on Mid-Atlantic Offshore Wind and Implications for Wind Resource Assessment: A Case Study. *Journal of Applied Meteorology and Climatology*, 57, 3, 777–796. Doi:10.1175/JAMC-D-17-0143.1

Sweet, W., Dusek, G., Carbin, G., Marra, J., Marcy, D., and Simon, S. (2020). 2019 State of U.S. High Tide Flooding with a 2020 Outlook. NOAA Technical Report NOS CO-OPS 092, 24 pp.

Sweet, W. V., Dusek, G., Obeysekera, J., and Marra, J. J. (2018). Patterns and Projections of High Tide Flooding Along the U.S. Coastline Using a Common Impact Threshold. NOAA Technical Report NOS CO-OPS 086, 56 pp.

Sweet, W. V., Horton, R. M., Kopp, R. E., LeGrande, A. N., and Romanou, A. (2017a). Sea level rise. In: Climate Science Special Report: Fourth National Climate Assessment, Volume I [Wuebbles, D.J., D.W. Fahey, K.A. Hibbard, D.J. Dokken, B.C. Stewart, and T.K. Maycock (eds.)]. U.S. Global Change Research Program, Washington, DC, USA, pp. 333-363. doi:10.7930/J0VM49F2.

Sweet, W. V., Kopp, R. E., Weaver, C. P., Obeysekera, J., Horton, R. M., Thieler, E. R., and Zervas, C. (2017b). Global and Regional Sea Level Rise Scenarios for the United States. NOAA Technical Report NOS CO-OPS 083, 75 pp.

Sweet, W. V., Park, J., Marra, J. J., Zervas, C. E., and Gill, S. (2014). Sea Level Rise and Nuisance Flood Frequency Changes around the United States. NOAA Technical Report NOS CO-OPS 073, 66 pp.

Tebaldi, C., Strauss, B. H., and Zervas, C. E. (2012). Modeling sea level rise impacts on storm surges along US coasts. *Environmental Research Letters*, 7, 014032.

Thompson, R. O. R. Y. (1983). Low-pass filters to suppress inertial and tidal frequencies. *Journal of Physical Oceanography*, 13, 1077-1083.

Thompson, P. R., Mitchum, G. T., Vonesch, C., and Li, J. (2013). Variability of Winter Storminess in the Eastern United States during the Twentieth Century from Tide Gauges, *Journal of Climate*, 26, 9713-9726. doi:10.1175/JCLI-D-12-00561.1

[USACE] US Army Corps of Engineers. (2014). North Atlantic Coast Comprehensive Study (NACCS), State Chapter D-7: State of Delaware, 142 pp.

Wilkerson, C. N., and Brubaker, J. (2013). Analysis of Extreme Water Levels in the Lower Chesapeake Bay. *Proceedings of the 2012 OCEANS Conference*, Hampton Roads, VA. doi:10.1109/OCEANS.2012.6405098

Weinkle, J., Landsea, C., Collins, D., Musulin, R., Crompton, R. P., Klotzbach, P. K., and Pielke R. Jr (2018). Normalized hurricane damage in the continental United States 1900–2017. *Nature Sustainability*. doi:10.1038/s41893-018-0165-2

Williams, J., Horsburgh, K. J., Williams, J. A., and Proctor, R. N. F. (2016). Tide and skew surge independence: New insights for flood risk. *Geophysical Research Letters*, 43, 6410–6417. doi:10.1002/2016GL069522

Wong, K–C., and Münchow, A. (1995). Buoyancy forced interaction between estuary and inner shelf: observation. *Continental Shelf Research*, 15:1, 59-88.

[WMO] World Meteorological Organization. (2020). Tropical Cyclone Naming, website. https://public.wmo.int/en/our-mandate/focus-areas/natural-hazards-and-disaster-risk-reduction/tropical-cyclones/Naming [Accessed August 15, 2020].

Xie, L., Yan, T., Pietrafesa, L. J., Morrison, J. M., and Karl, T. (2005). Climatology and interannual variability of North Atlantic hurricane tracks. *Journal of Climate*, 18, 5370-5381.

Xiong, Y. and Berger, C. R. (2010). Chesapeake Bay Tidal Characteristics. *Journal of Water Resource and Protection*, 2, 619-628. doi:10.4236/jwarp.2010.27071

Yang, H., Lohmann, G., Lu, J., Gowan, E.J., Shi, X., Liu, J., Wang, Q. (2020). Tropical expansion driven by poleward advancing mid-latitude meridional temperature gradients. *JGR Atmospheres*. doi:10.1029/2020JD033158

Zhang, K., Douglas, B. C., and Leatherman, S. P. (2000). Twentieth-Century Storm Activity along the U.S. East Coast. *Journal of Climate*, 13, 1748-1761.

Zhong, L., and Li, M. (2006). Tidal Energy Fluxes and Dissipation in the Chesapeake Bay. *Continental Shelf Research*, 26, 6, 752-770.

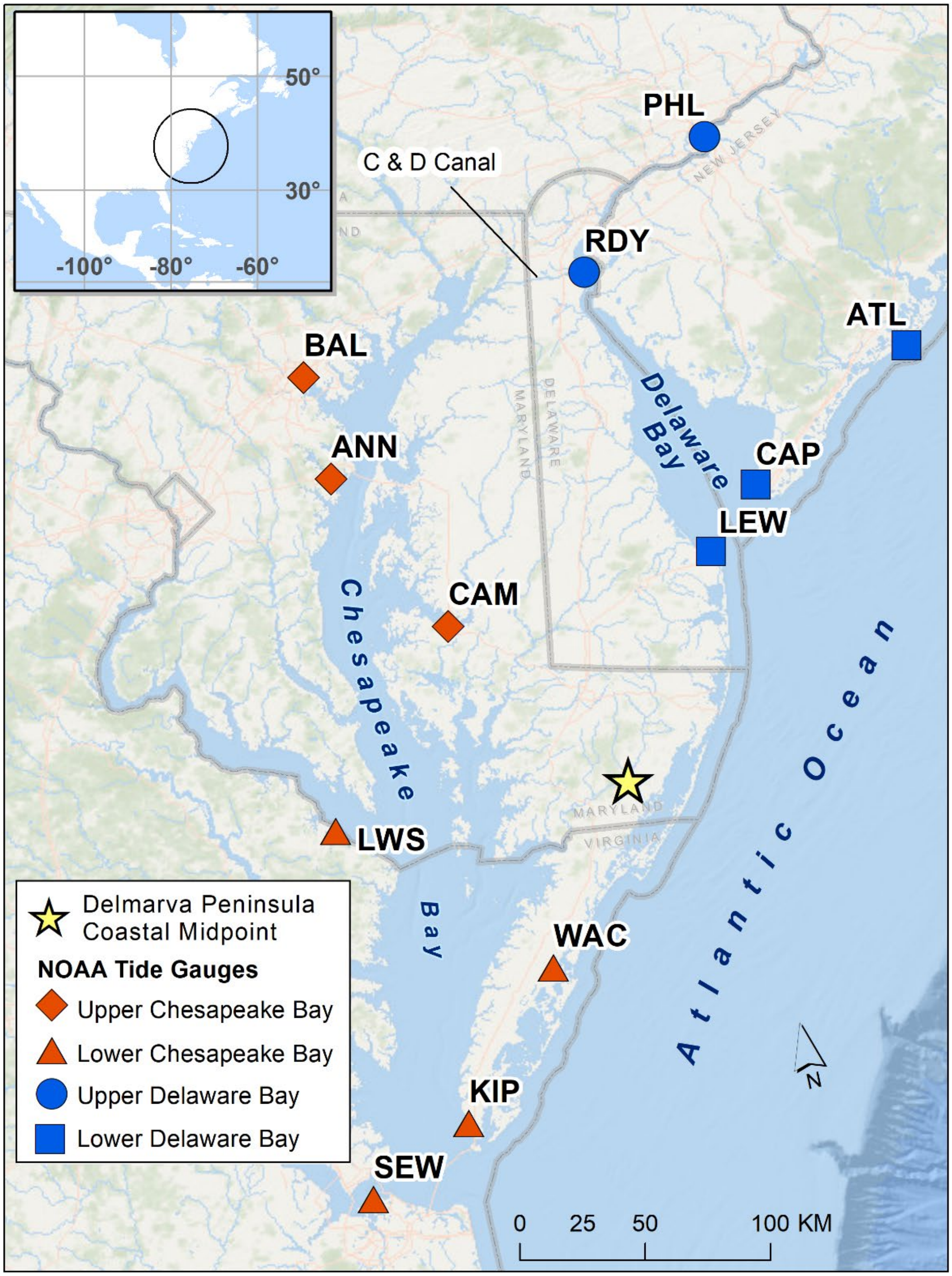

Figure 1. Map of the Delaware and Chesapeake Bays highlighting NOAA tide gauges used in the current study. The inset overview map shows the 750 km circular buffer around the Delmarva Peninsula reference point (yellow star in the main map) computed from the mean latitude and longitude of the six ocean coastal gauges, namely Atlantic City (ATL), Cape May (CAP), Lewes (LEW), Wachapreague (WAC), Kiptopeke (KIP), and Sewells Point (SEW).

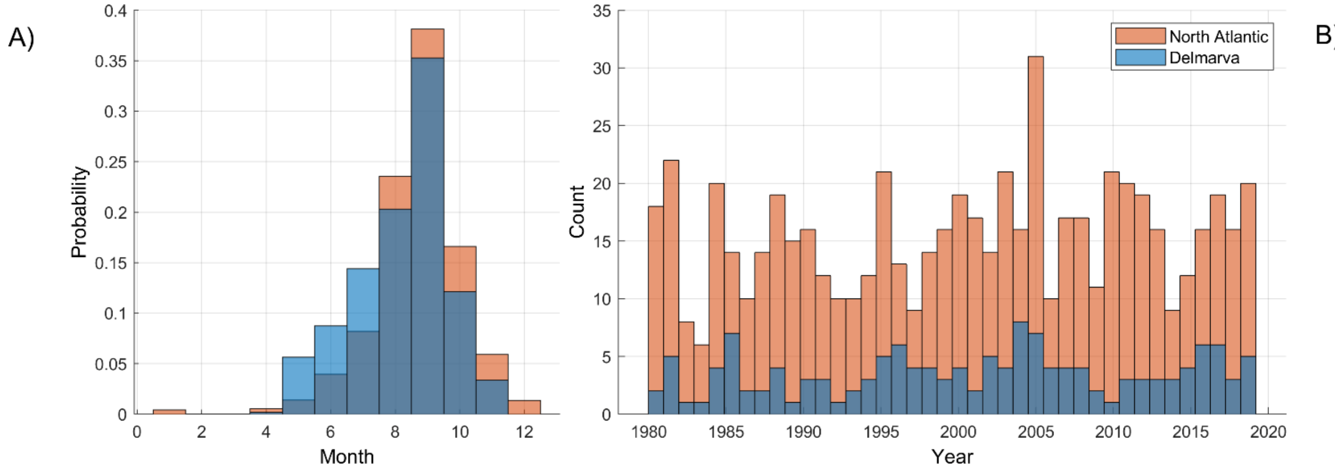

Figure 2. Seasonal (a) and annual (b) distribution of all North Atlantic tropical cyclones and the subset of those that cross 750 km buffer around Delmarva Peninsula, 1980 – 2019.

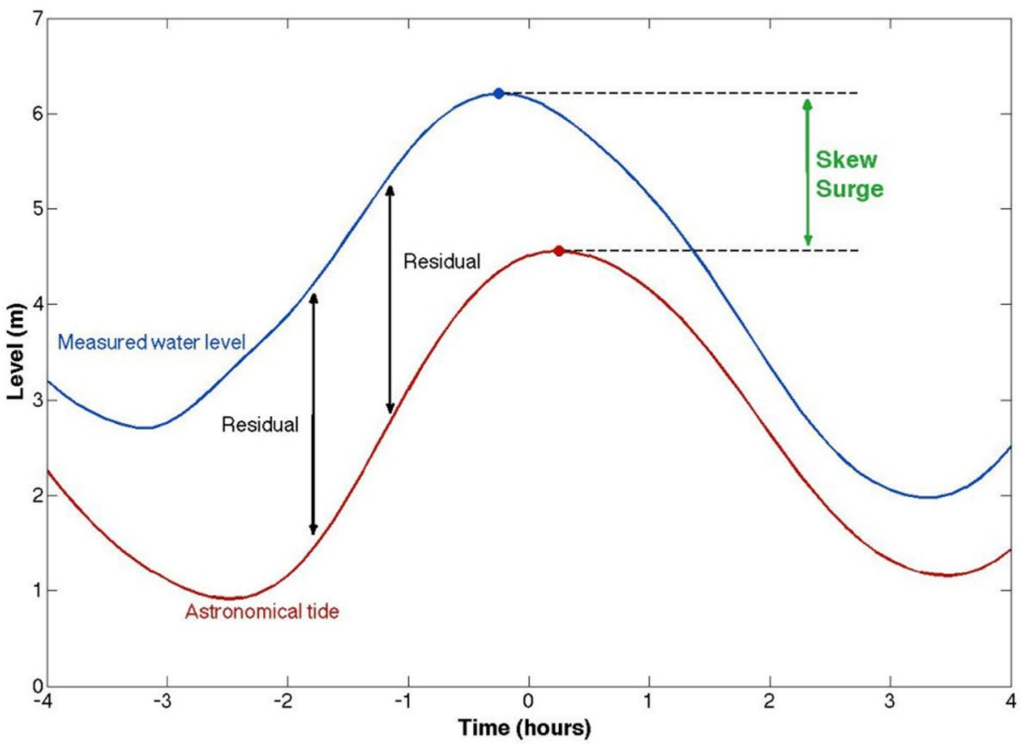

Figure 3. Diagram of skew surge during a tidal cycle. In the above example, the total water level and predicted tide peaks are skewed from one another. The maximum non-tidal residual (difference between observed total water level and predicted tide) occurs closer to low tide than to high tide peak. (Source: Mawdsley and Haigh, 2016.)

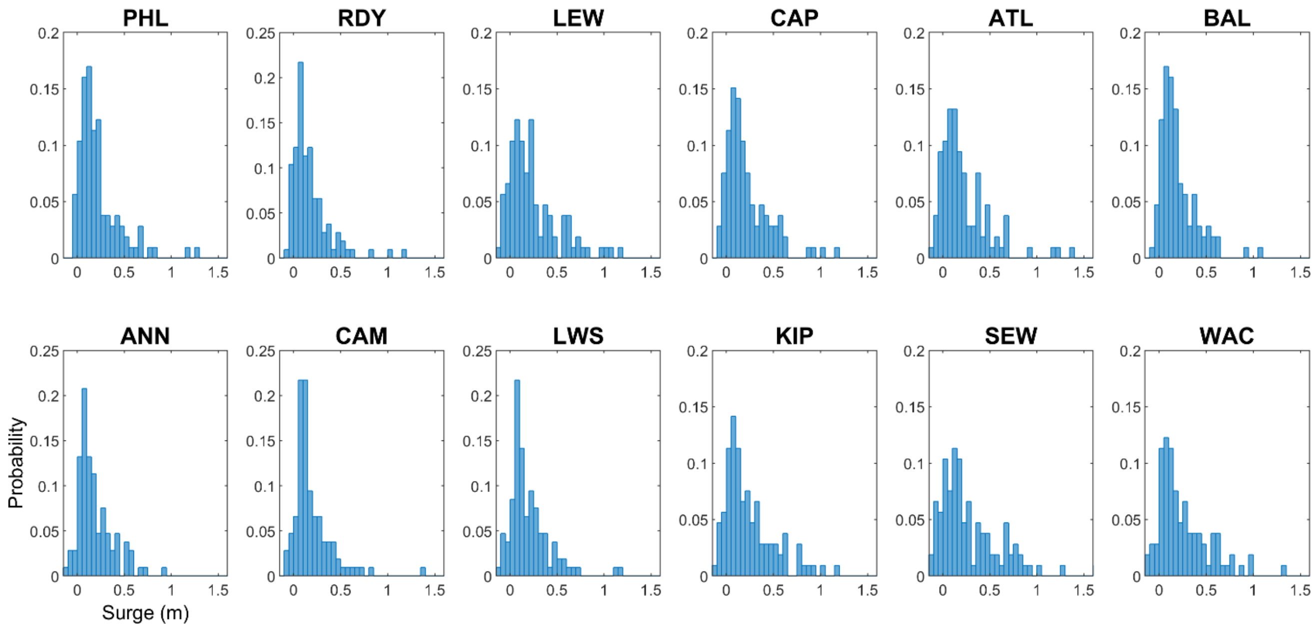

Figure 4. Distribution of skew surge for Delmarva tropical cyclones, 1980 – 2019. Values in meters.

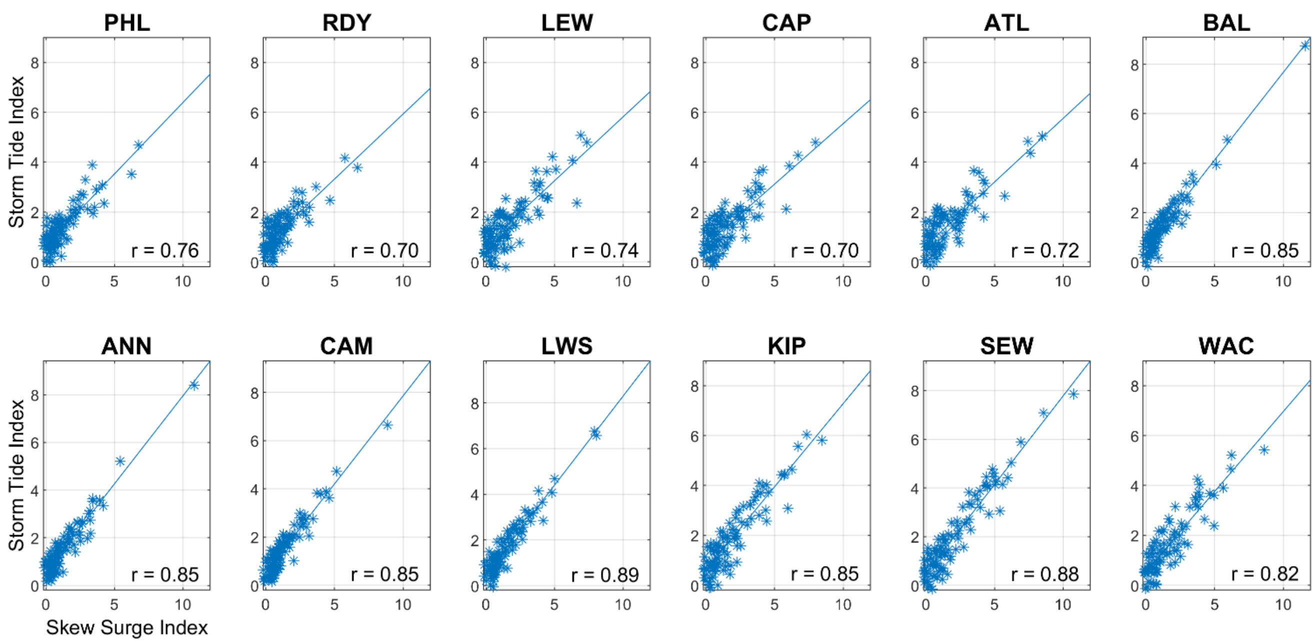

Figure 5. Scatterplot and regression line of skew surge index (SSI) against storm tide index (STI) for Delmarva tropical cyclones, 1980 – 2019. Regression line based on least squares method.

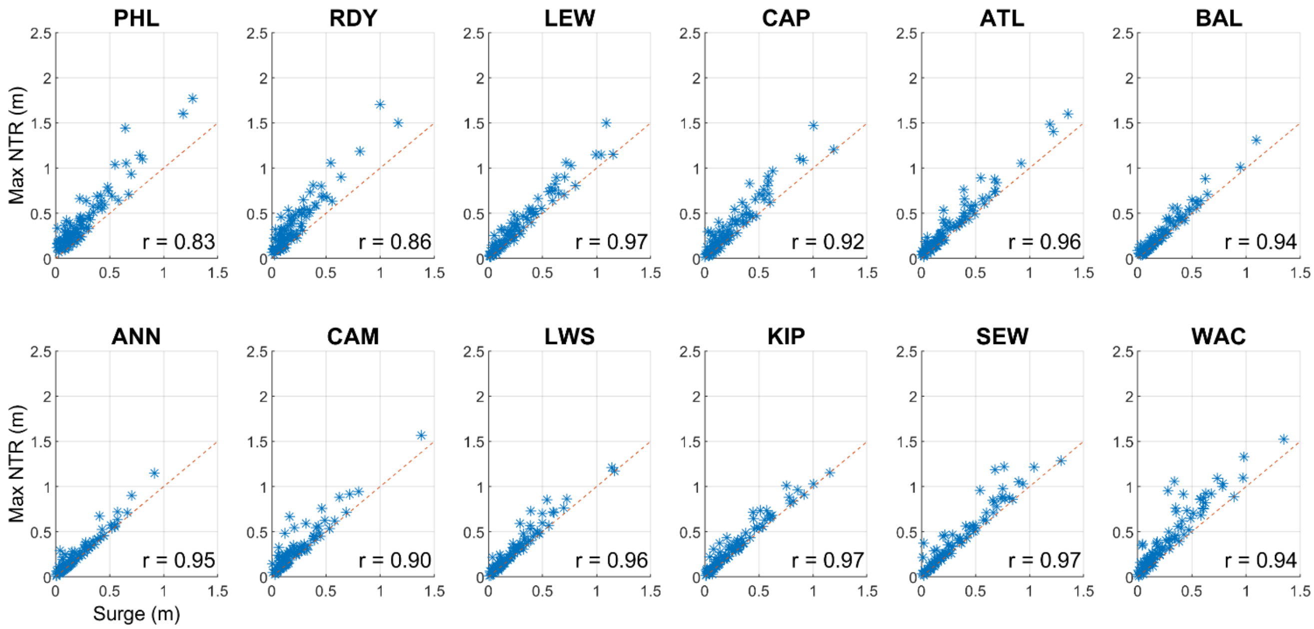

Figure 6. Scatterplot and 1:1 ratio line of skew surge against maximum non-tidal residual (NTR) for Delmarva tropical cyclones, 1980 – 2019. Values in meters.

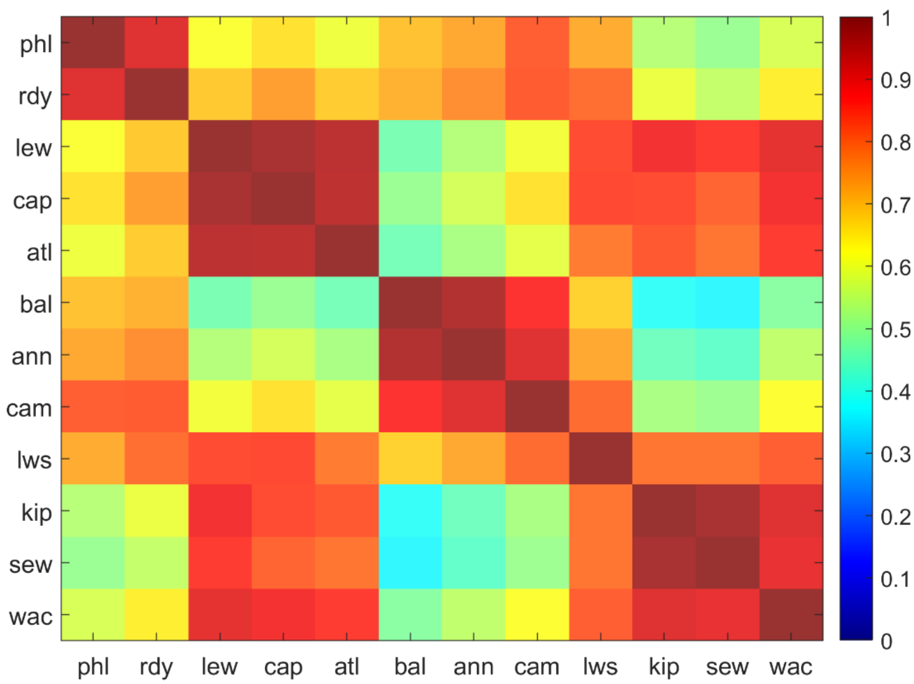

Figure 7. Corrgram of cross-correlation of skew surge index (SSI) for Delmarva tropical cyclones, 1980 - 2019. Correlation values computed using Spearman Rank method. Red (blue) colors represent higher (lower) correlations. Regions of gauges with similar correlations are easily identifiable as like colors. All correlations are statistically significant at p = 0.01 level.

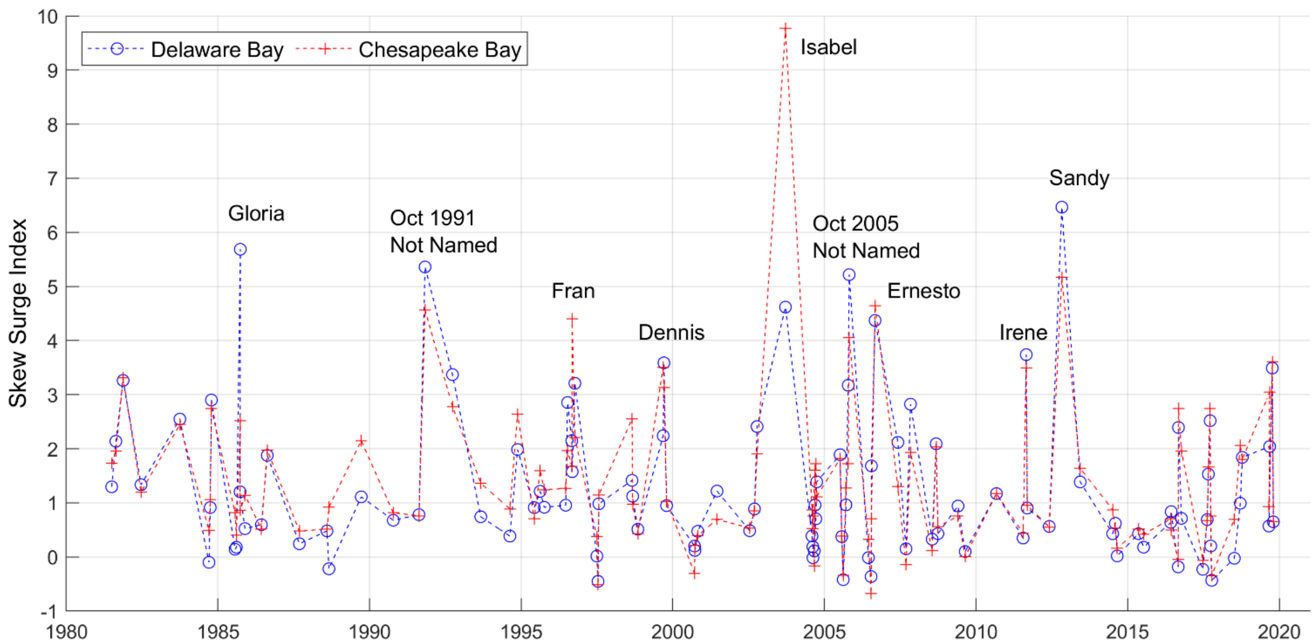

Figure 8. Skew surge index (SSI) for Delmarva tropical cyclones averaged over gauges within the Delaware (blue) and Chesapeake (red) Bays, 1980 – 2019.

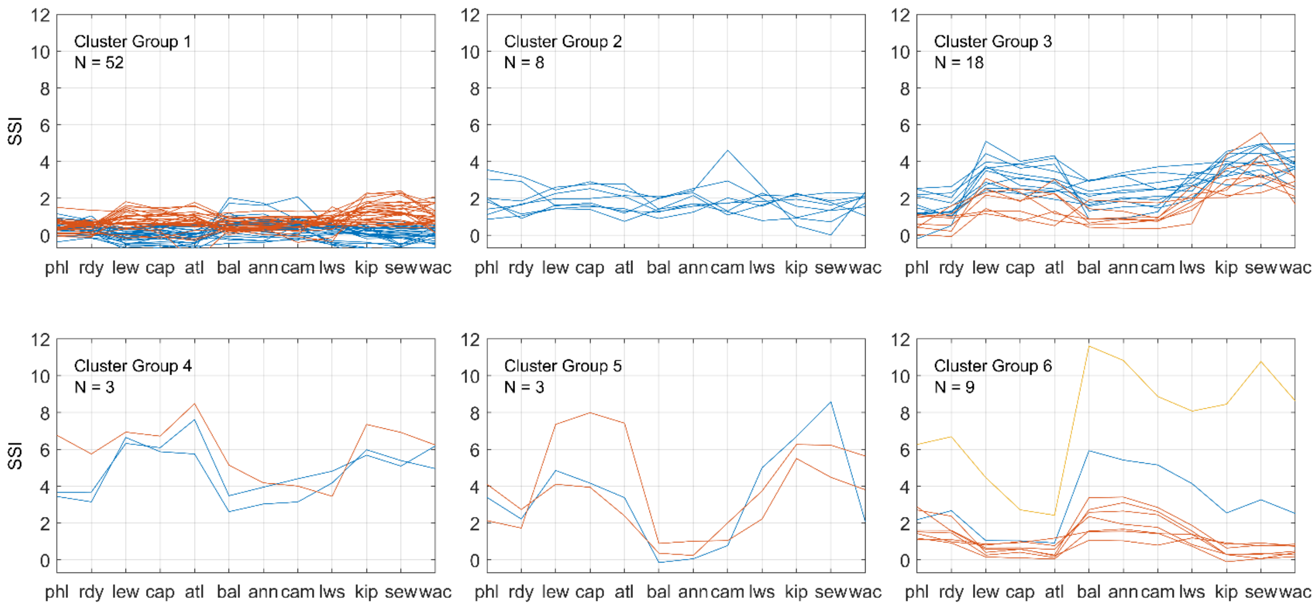

Figure 9. A-F. K-Means clusters of Delmarva tropical cyclone (TC) storm tracks, 1980 – 2019. Clustering based on spatial pattern of skew surge index (SSI) across 12 gauges in study region. 12 clusters are identified with the number of TCs in each cluster labelled on the plots. Some clusters were grouped together in the panels above based on similar spatial pattern of surge.

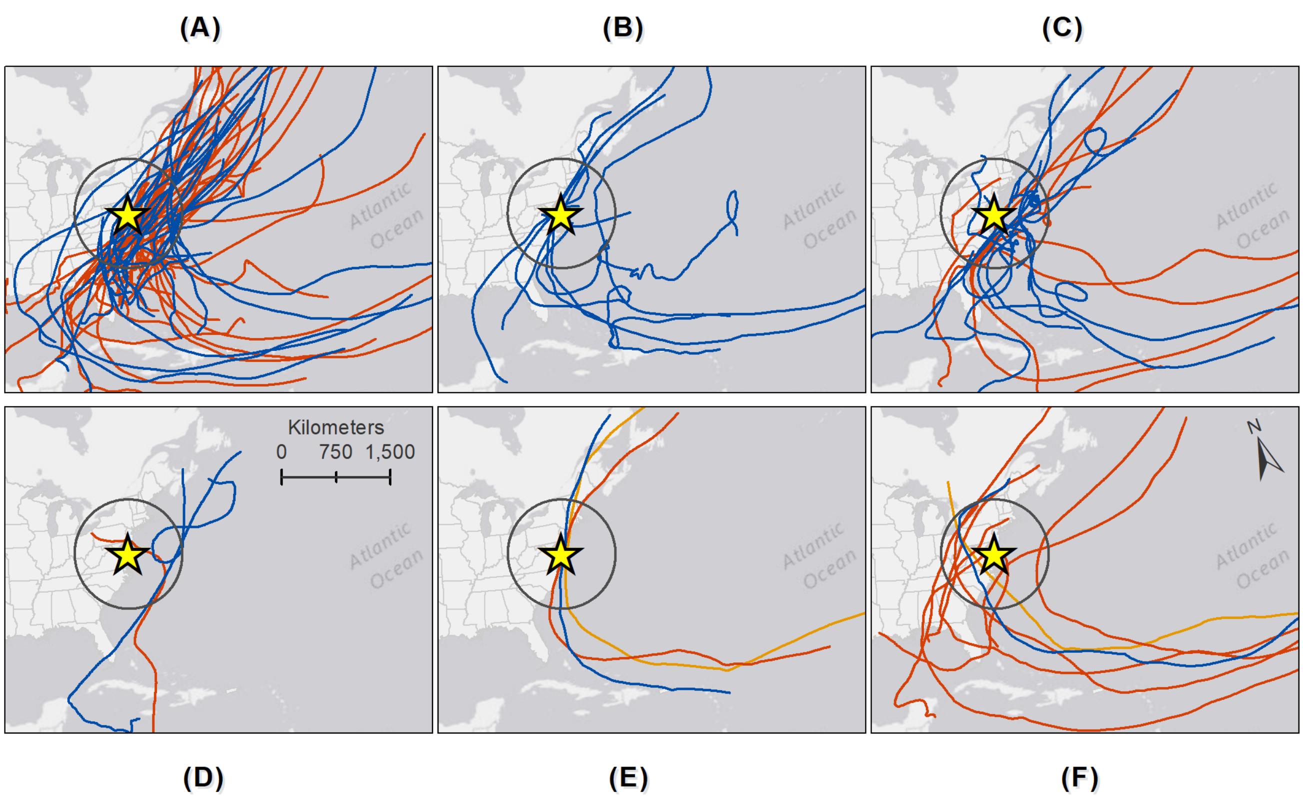

Figure 10. A-F. Individual tracks of K-Means clusters of Delmarva tropical cyclones (TCs), 1980 – 2019. Each panel map corresponds to the same panel of skew surge index (SSI) profiles plotted in Figure 9.

Supplementary Material

1. Supplementary Figures

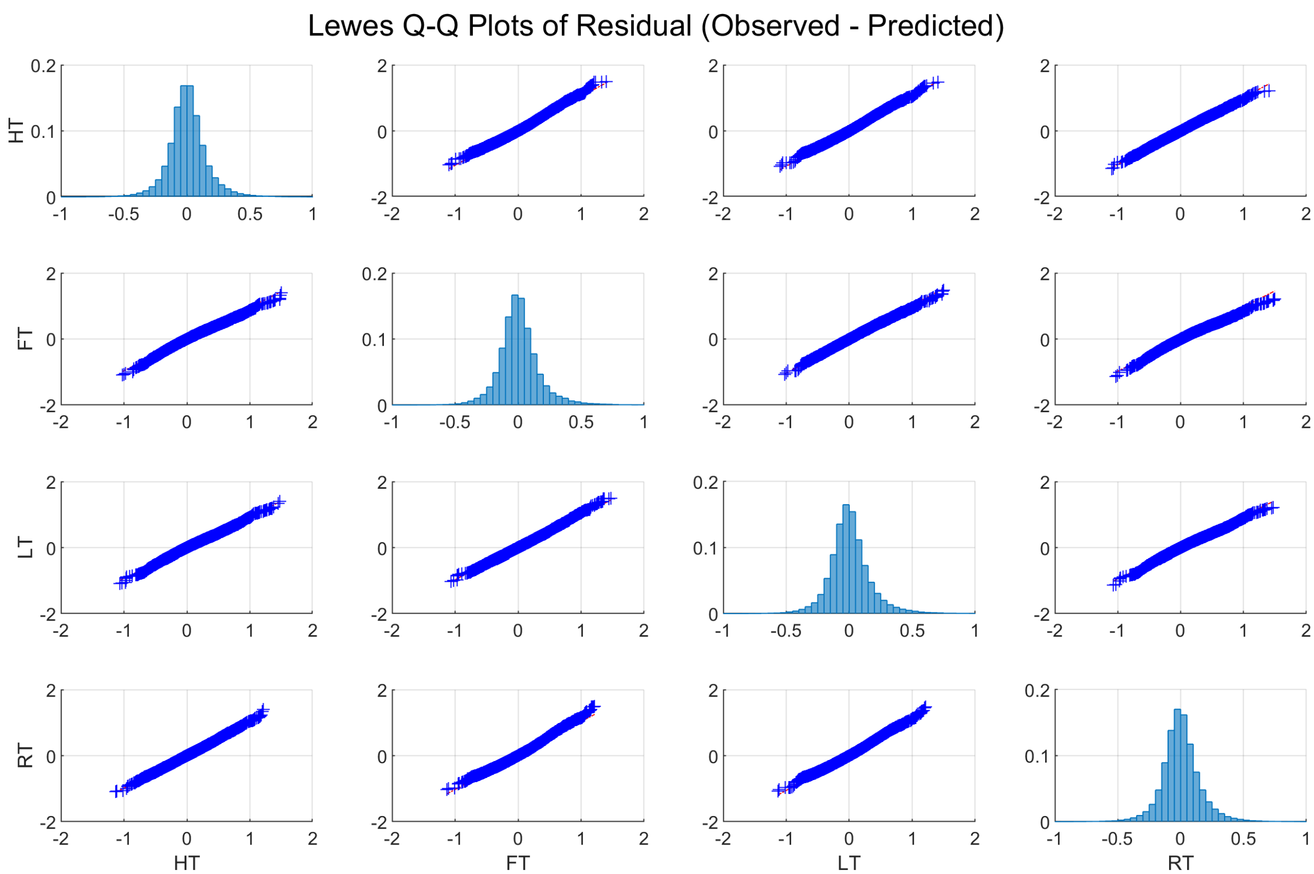

Supplementary Figure 1. Quantile-Quantile plot of hourly residual water levels (observed minus predicted) for the NOAA Lewes tide gauge in the Lower Delaware Bay for 1980 – 2019. Residuals were divided into four time periods based on tidal phase: High Tide (HT), Falling Tide (FT), Low Tide (LT), and Rising Tide (RT). High and Low time periods were defined as 1.5 hours before and after tidal peak. Diagonals show histogram plots in 0.05 m bins for each tidal phase over the same time period. Data show strong agreement with the Normal distribution. Anderson-Darling test statistic is near zero for all comparisons between distributions of each phase. These data at Lewes are representative of gauges within the Delaware and Chesapeake Bays.

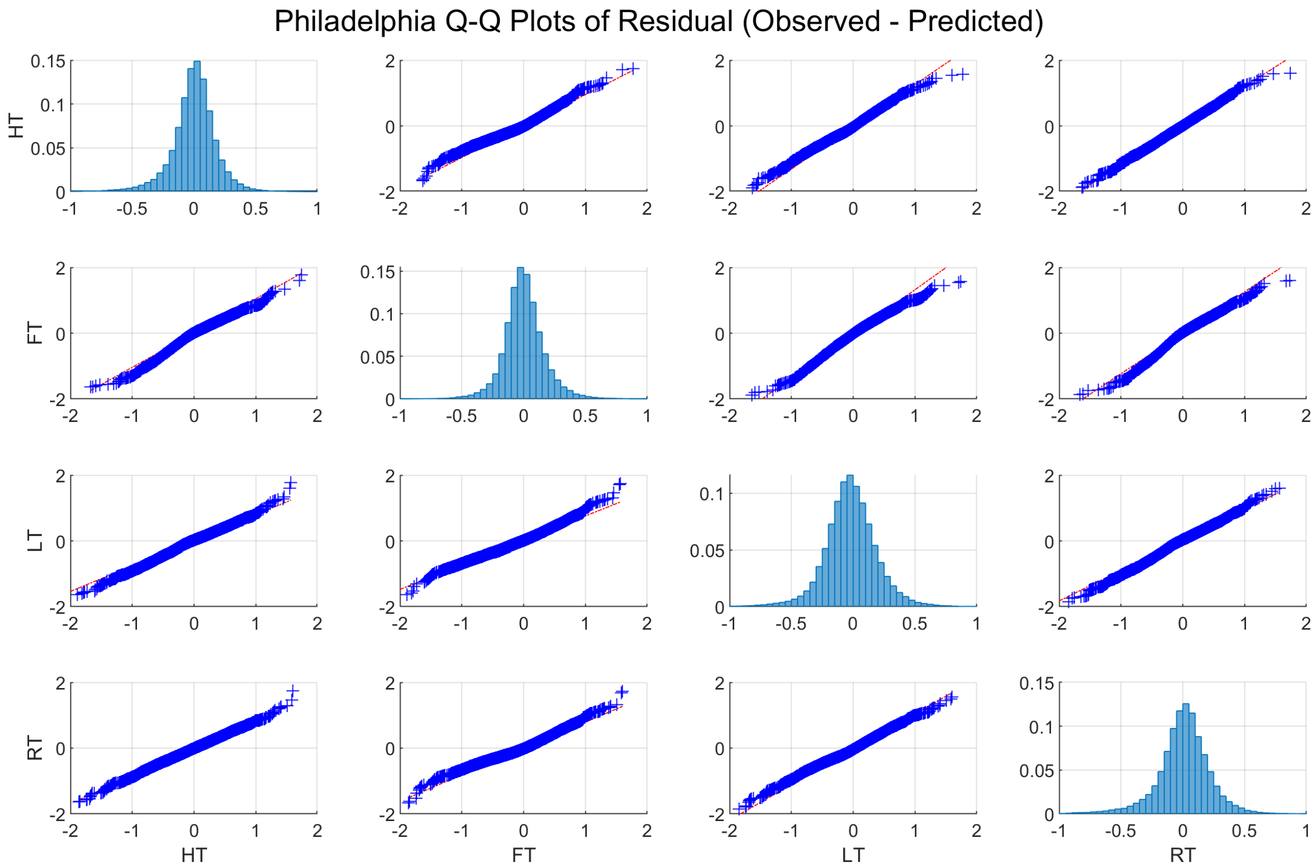

Supplementary Figure 2. Quantile-Quantile plot of hourly residual water levels (observed minus predicted) for the NOAA Philadelphia tide gauge in the Upper Delaware Bay for 1980 – 2019. Residuals were divided into four time periods based on tidal phase: High Tide (HT), Falling Tide (FT), Low Tide (LT), and Rising Tide (RT). High and Low time periods were defined as 1.5 hours before and after tidal peak. Diagonals show histogram plots in 0.05 m bins for each tidal phase over the same time period. Data show strong agreement with the Normal distribution. Although these data at Baltimore show the most variation away from a perfect 1:1 fit at the extremes between each phase, the Anderson-Darling test statistic is near zero for all comparisons between distributions of each phase. Other upper bay gauges show characteristics that are between what is shown at Lewes and Baltimore.

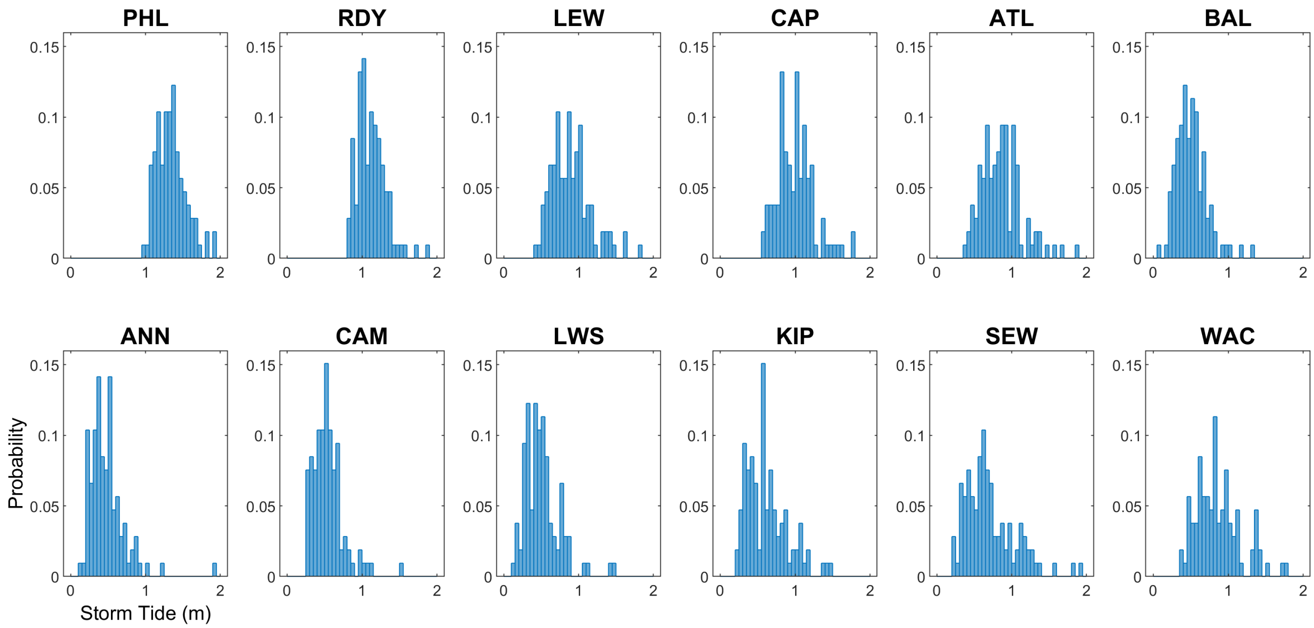

Supplementary Figure 3. Histogram distribution of storm tide for Delmarva TCs, 1980 – 2019. Values are in meters relative to NAVD88 datum.

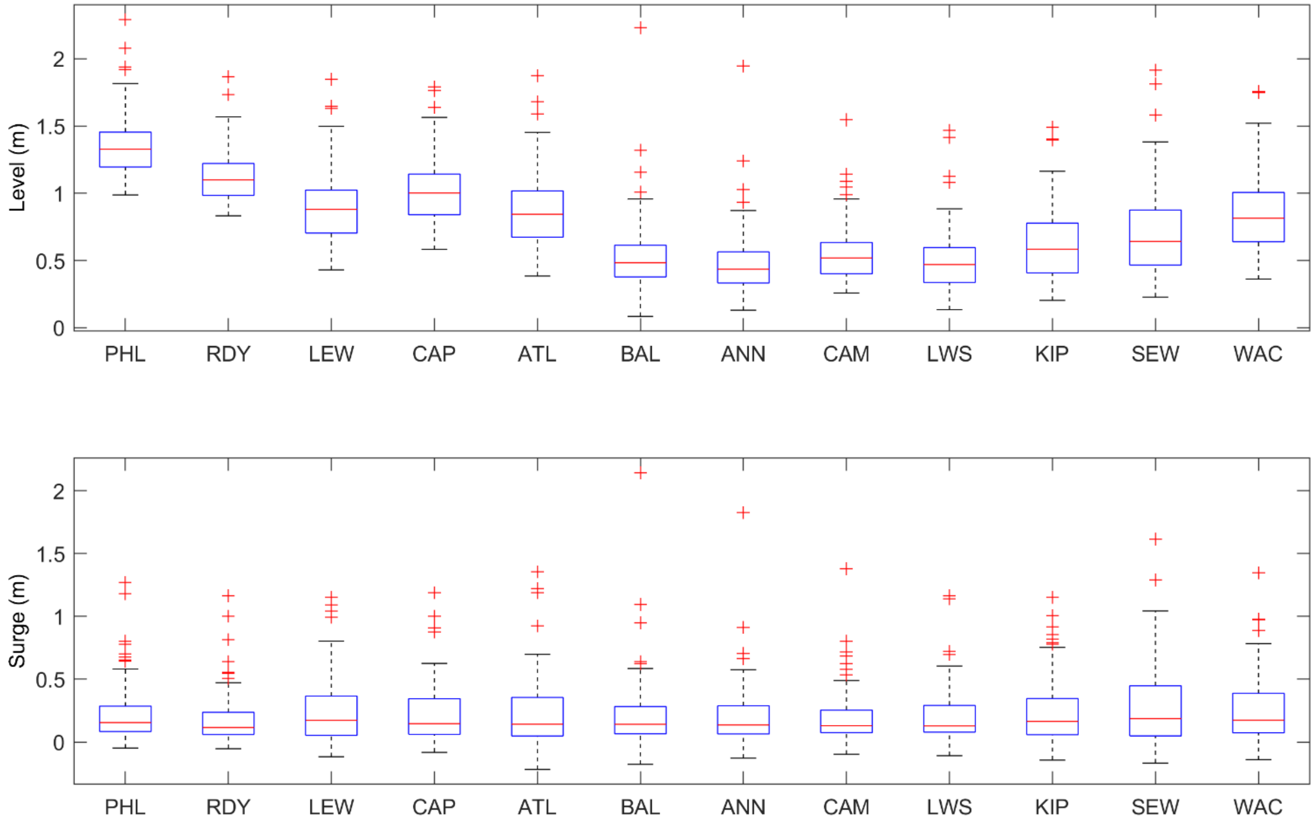

Supplementary Figure 4. Box plots of storm tide and skew surge for Delmarva TCs, 1980 – 2019. Plus signs above the top hash marks represent storms with values greater than 1.5 times the interquartile range. Values are in meters. Storm tides are meters relative to NAVD88 datum. Box plots more clearly show differences in mean water levels and extent of extremes among gauges.

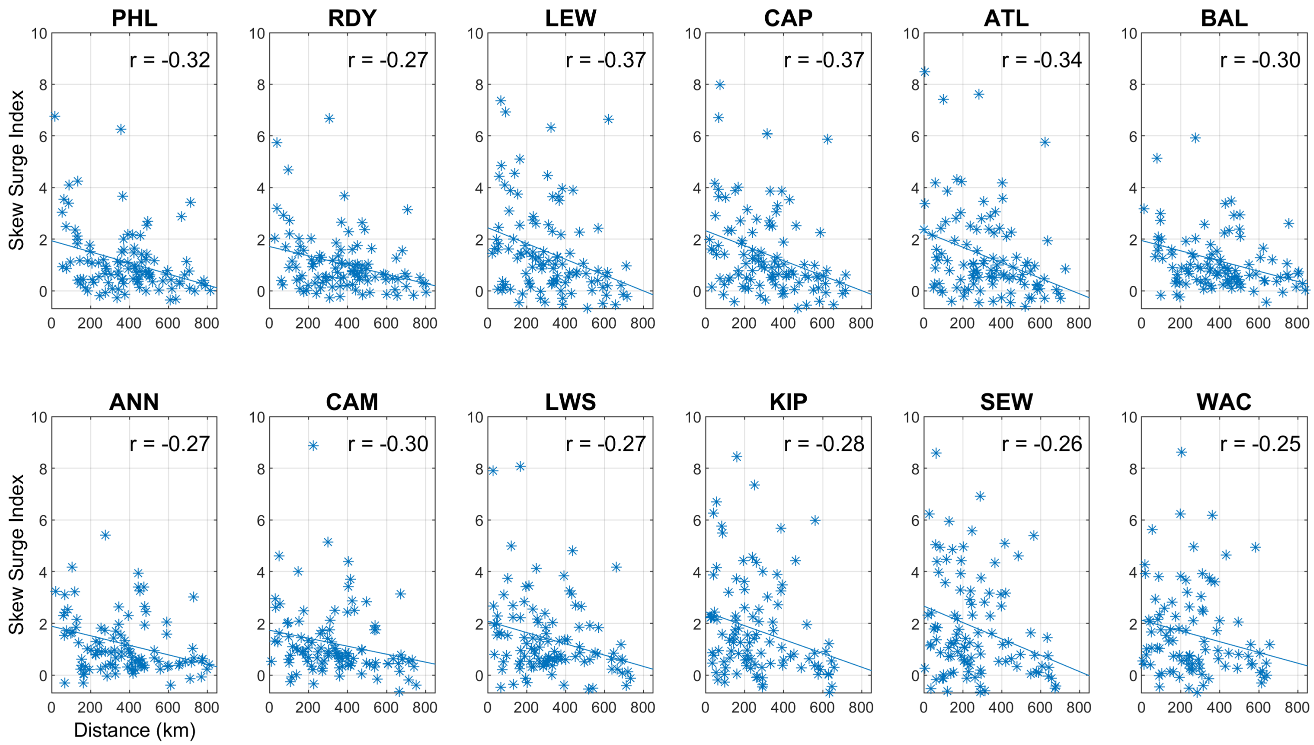

Supplementary Figure 5. Scatterplot and regression line of best fit of skew surge index (SSI) against minimum distance of Delmarva TC's, 1980 – 2019. Regression line computed based least squares method. All correlations significant at the p = 0.01 level.

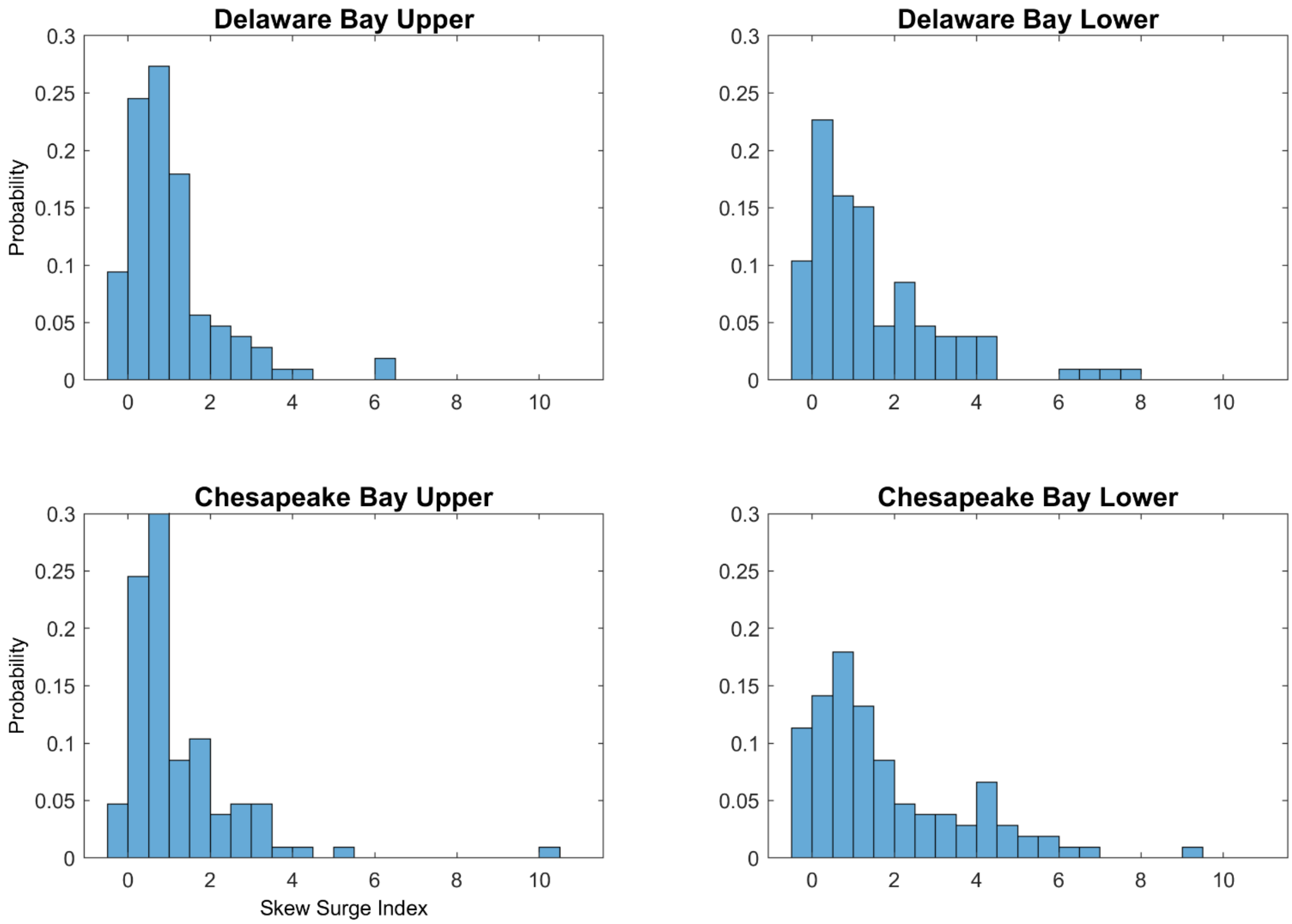

Supplementary Figure 6. Histogram distributions of skew surge index of Delmarva tropical cyclones (N = 106) for Delaware and Chesapeake Bay regions, 1980 – 2019.

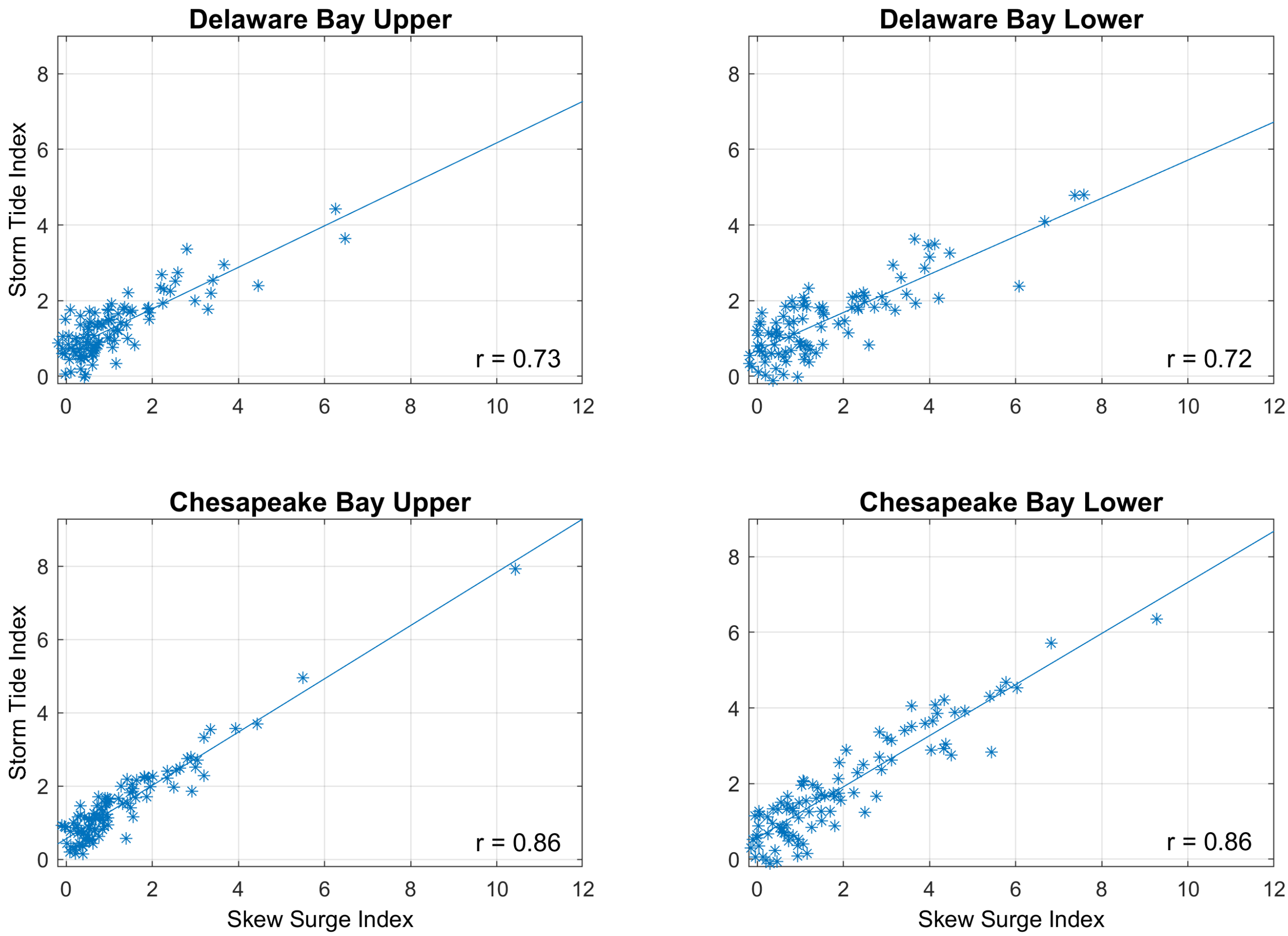

Supplementary Figure 7. Skew surge index plotted against storm tide index for Delmarva tropical cyclones (N = 106) for Delaware and Chesapeake Bay regions, 1980 – 2019. All correlations statistically significant at $p = 0.01$ level.

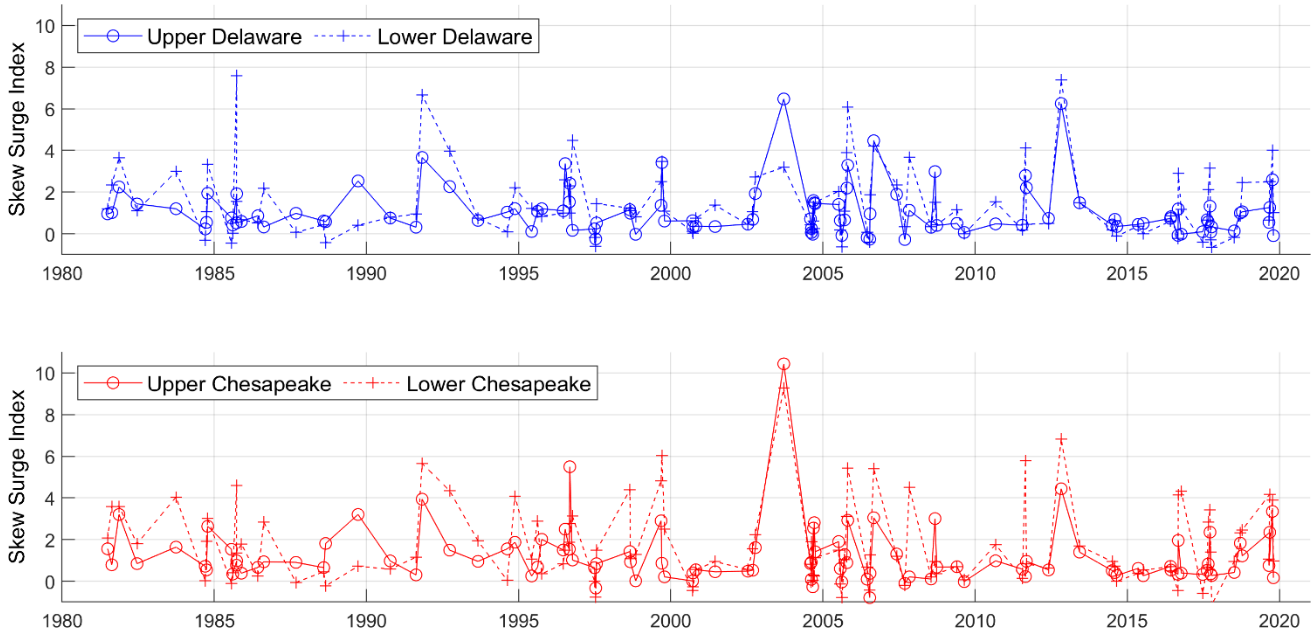

Supplementary Figure 8. Skew surge index (SSI) for Delmarva tropical cyclones averaged over all gauges within each geographic region of Delaware (blue) and Chesapeake (red) Bays, 1980 – 2019. Solid lines with circles represent upper bays; dashed lines with plus signs represent lower bays.

2. Supplementary Tables

Supplementary Table 1. Cross-correlation coefficients comparing storm tide index (i.e., detrended and normalized storm tide) among all 12 NOAA tide gauges within the Delaware and Chesapeake Bay regions for Delmarva tropical cyclones, 1980 - 2019. Correlations were computed pairwise using Spearman Rank correlation method. All correlations are statistically significant at p = 0.01 level. Shaded cells highlight groups of gauges with unusually high correlations within the same geographic region.

	Storm Tide Index (STI) Cross-Correlation											
Station	**PHL**	**RDY**	**LEW**	**CAP**	**ATL**	**BAL**	**ANN**	**CAM**	**LWS**	**KIP**	**SEW**	**WAC**
PHL	1.00	0.93	0.67	0.70	0.65	0.63	0.64	0.74	0.65	0.52	0.42	0.56
RDY	0.93	1.00	0.73	0.76	0.71	0.66	0.67	0.76	0.71	0.57	0.47	0.63
LEW	0.67	0.73	1.00	0.97	0.94	0.39	0.44	0.57	0.75	0.87	0.80	0.91
CAP	0.70	0.76	0.97	1.00	0.96	0.41	0.44	0.58	0.68	0.79	0.70	0.84
ATL	0.65	0.71	0.94	0.96	1.00	0.34	0.39	0.51	0.61	0.76	0.67	0.80
BAL	0.63	0.66	0.39	0.41	0.34	1.00	0.97	0.88	0.64	0.30	0.26	0.41
ANN	0.64	0.67	0.44	0.44	0.39	0.97	1.00	0.90	0.69	0.36	0.32	0.47
CAM	0.74	0.76	0.57	0.58	0.51	0.88	0.90	1.00	0.78	0.49	0.45	0.60
LWS	0.65	0.71	0.75	0.68	0.61	0.64	0.69	0.78	1.00	0.78	0.77	0.79
KIP	0.52	0.57	0.87	0.79	0.76	0.30	0.36	0.49	0.78	1.00	0.97	0.91
SEW	0.42	0.47	0.80	0.70	0.67	0.26	0.32	0.45	0.77	0.97	1.00	0.87
WAC	0.56	0.63	0.91	0.84	0.80	0.41	0.47	0.60	0.79	0.91	0.87	1.00

Supplementary Table 2. Cross-correlation coefficients comparing skew surge index (i.e., detrended and normalized skew surge) among all 12 NOAA tide gauges in the Delaware and Chesapeake Bays regions for Delmarva tropical cyclones, 1980 - 2019. Correlations were computed pairwise using Spearman Rank correlation method. All correlations are statistically significant at p = 0.01 level. Shaded cells highlight groups of gauges with unusually high correlations within the same geographic region.

	Skew Surge Index (SSI) Cross-Correlation											
Station	**PHL**	**RDY**	**LEW**	**CAP**	**ATL**	**BAL**	**ANN**	**CAM**	**LWS**	**KIP**	**SEW**	**WAC**
PHL	1.00	0.91	0.61	0.66	0.60	0.70	0.73	0.82	0.73	0.54	0.50	0.57
RDY	0.91	1.00	0.69	0.74	0.68	0.72	0.76	0.82	0.80	0.60	0.55	0.64
LEW	0.61	0.69	1.00	0.98	0.96	0.46	0.53	0.61	0.84	0.89	0.86	0.90
CAP	0.66	0.74	0.98	1.00	0.95	0.50	0.57	0.66	0.84	0.84	0.81	0.88
ATL	0.60	0.68	0.96	0.95	1.00	0.46	0.52	0.59	0.78	0.83	0.79	0.86
BAL	0.70	0.72	0.46	0.50	0.46	1.00	0.97	0.88	0.68	0.38	0.37	0.48
ANN	0.73	0.76	0.53	0.57	0.52	0.97	1.00	0.91	0.73	0.45	0.44	0.55
CAM	0.82	0.82	0.61	0.66	0.59	0.88	0.91	1.00	0.80	0.52	0.50	0.62
LWS	0.73	0.80	0.84	0.84	0.78	0.68	0.73	0.80	1.00	0.79	0.79	0.82
KIP	0.54	0.60	0.89	0.84	0.83	0.38	0.45	0.52	0.79	1.00	0.98	0.91
SEW	0.50	0.55	0.86	0.81	0.79	0.37	0.44	0.50	0.79	0.98	1.00	0.90
WAC	0.57	0.64	0.90	0.88	0.86	0.48	0.55	0.62	0.82	0.91	0.90	1.00

Supplementary Table 3. Delmarva tropical cyclones with the largest difference in skew surge index (SSI) between the Delaware and Chesapeake Bays, 1980 – 2019. Diff column is the absolute value of the difference in SSI. Year and Month note the time of storm's closest approach to Delmarva. Status represents the most common value of USA_STATUS attribute in the IBTrACS database while the storm is within the 750 km buffer. EX = Extratropical, HU = Hurricane, TS = Tropical Storm, TD = Tropical Depression, SS = Subtropical Storm, DB = Disturbance. Refer to the IBTrACS Version 4 Technical Documentation for more details.

	Delaware Bay > Chesapeake Bay SSI						**Chesapeake Bay > Delaware Bay SSI**				
Rank	**Name**	**Yr**	**Mon**	**Status**	**Diff**		**Name**	**Yr**	**Mon**	**Status**	**Diff**
1	GLORIA	1985	9	HU	3.17		ISABEL	2003	9	HU	5.15
2	NOT_NAMED	2005	10	EX	1.45		FRAN	1996	9	TD	2.83
3	SANDY	2012	10	EX	1.29		DENNIS	1999	9	TS	1.27
4	WILMA	2005	10	HU	1.17		MATTHEW	2016	10	HU	1.24
5	JOSEPHINE	1996	10	EX	1.00		BONNIE	1998	8	HU	1.14
6	BERYL	2006	7	TS	0.98		CHRIS	1988	8	EX	1.14
7	NOEL	2007	11	EX	0.90		FLORENCE	2018	9	HU	1.07
8	BERTHA	1996	7	TS	0.89		HUGO	1989	9	HU	1.04
9	BARRY	2007	6	EX	0.82		IVAN	2004	9	EX	1.02
10	NOT_NAMED	1991	10	EX	0.80		DORIAN	2019	9	HU	1.01

Supplementary Table 4. Top 25 Delmarva tropical cyclones, ranked by skew surge index (SSI), for the Upper and Lower Delaware Bay, 1980 – 2019. Year and Month note the time of storm's closest approach to Delmarva. Status represents the most common value of USA_STATUS attribute in the IBTrACS database while the storm is within the 750 km buffer. EX = Extratropical, HU = Hurricane, TS = Tropical Storm, TD = Tropical Depression, SS = Subtropical Storm, DB = Disturbance. Refer to the IBTrACS Version 4 Technical Documentation for more details.

	Upper Delaware Bay					Lower Delaware Bay			
Rank	**Name**	**Year**	**Month**	**Status**		**Name**	**Year**	**Month**	**Status**
1	ISABEL	2003	9	HU		GLORIA	1985	9	HU
2	SANDY	2012	10	EX		SANDY	2012	10	EX
3	ERNESTO	2006	9	EX		NOT_NAMED	1991	10	EX
4	NOT_NAMED	1991	10	EX		WILMA	2005	10	HU
5	FLOYD	1999	9	HU		JOSEPHINE	1996	10	EX
6	BERTHA	1996	7	TS		ERNESTO	2006	9	EX
7	WILMA	2005	10	HU		IRENE	2011	8	HU
8	HANNA	2008	9	TS		MELISSA	2019	10	EX
9	IRENE	2011	8	HU		DANIELLE	1992	9	TS
10	MELISSA	2019	10	EX		NOT_NAMED	2005	10	EX
11	HUGO	1989	9	HU		NOEL	2007	11	EX
12	FRAN	1996	9	TD		NOT_NAMED	1981	11	SS
13	DANIELLE	1992	9	TS		FLOYD	1999	9	HU
14	NOT_NAMED	1981	11	SS		JOSEPHINE	1984	10	HU
15	KATIA	2011	9	HU		ISABEL	2003	9	HU
16	NOT_NAMED	2005	10	EX		JOSE	2017	9	TS
17	JOSEPHINE	1984	10	HU		DEAN	1983	9	TS
18	KYLE	2002	10	TS		HERMINE	2016	9	EX
19	GLORIA	1985	9	HU		KYLE	2002	10	TS
20	BARRY	2007	6	EX		BERTHA	1996	7	TS
21	FRANCES	2004	9	EX		DENNIS	1999	9	TS
22	EDOUARD	1996	9	HU		DORIAN	2019	9	HU
23	ANDREA	2013	6	EX		MICHAEL	2018	10	EX
24	IVAN	2004	9	EX		DENNIS	1981	8	TS
25	ISABEL	2003	9	HU		GLORIA	1985	9	HU

Supplementary Table 5. Same as Supplementary Table 4 except applied to Chesapeake Bay regions.

	Upper Chesapeake Bay					Lower Chesapeake Bay			
Rank	**Name**	**Year**	**Month**	**Status**		**Name**	**Year**	**Month**	**Status**
1	ISABEL	2003	9	HU		ISABEL	2003	9	HU
2	FRAN	1996	9	TD		SANDY	2012	10	EX
3	SANDY	2012	10	EX		FLOYD	1999	9	HU
4	NOT_NAMED	1991	10	EX		IRENE	2011	8	HU
5	MELISSA	2019	10	EX		NOT_NAMED	1991	10	EX
6	NOT_NAMED	1981	11	SS		WILMA	2005	10	HU
7	HUGO	1989	9	HU		ERNESTO	2006	9	EX
8	ERNESTO	2006	9	EX		DENNIS	1999	9	TS
9	HANNA	2008	9	TS		GLORIA	1985	9	HU
10	WILMA	2005	10	HU		NOEL	2007	11	EX
11	DENNIS	1999	9	TS		BONNIE	1998	8	HU
12	IVAN	2004	9	EX		DANIELLE	1992	9	TS
13	JOSEPHINE	1984	10	HU		MATTHEW	2016	10	HU
14	FRANCES	2004	9	EX		DORIAN	2019	9	HU
15	BERTHA	1996	7	TS		HERMINE	2016	9	EX
16	JOSE	2017	9	TS		GORDON	1994	11	HU
17	DORIAN	2019	9	HU		DEAN	1983	9	TS
18	OPAL	1995	10	EX		MELISSA	2019	10	EX
19	HERMINE	2016	9	EX		NOT_NAMED	1981	11	SS
20	CINDY	2005	7	EX		DENNIS	1981	8	TS
21	GORDON	1994	11	HU		JOSE	2017	9	TS
22	FLORENCE	2018	9	HU		JOSEPHINE	1996	10	EX
23	CHRIS	1988	8	EX		NOT_NAMED	2005	10	EX
24	DEAN	1983	9	TS		JOSEPHINE	1984	10	HU
25	ISABEL	2003	9	HU		ISABEL	2003	9	HU